Chapter 5
Image-Guided Radiation Therapy

X. Sharon Qi

Contents

5.1 Introduction

The goal of radiation therapy treatment is to deliver the therapeutic dose to target volumes while reduce the radiation exposure to the adjacent normal structures. In the past, a large three-dimensional planning margin was utilized to account for geometric and setup uncertainties, which resulted in unnecessary radiation doses to the surrounding normal tissues. Since the late 1990s, intensity-modulated radiation therapy (IMRT), which delivers highly conformal dose distributions to the target, has been widely adopted as standard treatment for treatment sites such as the head and neck, prostate, etc. (Butler et al. 1999; Manning et al. 2001; Zelefsky et al. 2000; De Meerleer et al. 2000). IMRT enables a more precise conformal radiation dose distribution to the target area without increasing radiation doses to the normal tissue. To translate the advantages of IMRT into better tumor control and reduction

X. Sharon Qi, PhD (✉)
Department of Radiation Oncology, University of California at Los Angeles, Los Angeles, CA, USA
e-mail: XQi@mednet.ucla.edu

M. Maqbool (ed.), *An Introduction to Medical Physics*, Biological and Medical Physics, Biomedical Engineering, DOI 10.1007/978-3-319-61540-0_5

of treatment-related toxicity, more accurate and reproducible patient setup is crucial (Qi et al. 2013a).

Recent developments in advanced treatment technology and medical imaging are essential for design of advanced treatment plans and to localize the target for precise administration of radiation. At planning stage, target definition is often based on CT, as well as other image modalities such as MRI and PET. At treatment stage, three-dimensional volumetric imaging can be used to localize the target and/or tumor motion. The changes in tumor position, size, and shape that take place during radiotherapy can be measured and accounted for to further improve geometric accuracy and precision of radiation delivery (Jaffray et al. 1999). By improving the accuracy of target delineation and treatment delivery through IGRT, radiation dose can be safely delivered to the target while reducing the doses to the surrounding healthy tissues resulting in better clinical outcome.

Image-guided radiation therapy (IGRT), broadly, involved any use of imaging to aid in decisions at various stages in the radiotherapy process: decision of whether and/or what to treat, delineation of range of interest in the planning process, aid in patient positioning, assessment of treatment outcome, etc. In the present context, the term IGRT signifies radiotherapy that used image-guidance procedures in two following aspects: (1) image-guided target delineation in radiation therapy and (2) image-guided treatment delivery. Target delineation refers to the use of advanced imaging modalities, including functional and/or biological images for target and normal structure delineation in RT planning. Imaged-guided treatment delivery refers to a process of frequent use of two-dimensional and/or three-dimensional imaging before, during, and/or after treatment using in-room technologies to guide radiation therapy. A wide variety of in-room IGRT modalities are available, such as matching planar kilovoltage (kV) radiographs or planar megavoltage (MV) images with digitally reconstructed radiographs (DRRs) from the planning CT and volumetric image technologies. An example of volumetric IGRT would include localization of a cone beam computed tomography (CBCT) dataset with the planning computed tomography (CT) dataset from planning. The IGRT procedures use imaging technology to identify and correct problems arising from inter- and intra-fractional variations in patient setup and anatomy, including shapes and volumes of treatment target, organ at risk, and surrounding normal tissues. IGRT is widely used for almost all treatment sites, i.e., prostate, head and neck, brain, lung, liver, etc.

5.2 Rationale for IGRT

Radiation therapy is considered as a local treatment that is designed to treat the defined targets in a specific area while sparing the surrounding normal tissue from receiving doses above specified dose tolerances. However, the doses delivered can be very different from the planned dose. There are many factors that may contribute to the dose deviations between the planned and the delivered dose distribution.

Among all, one important factor is patient setup error. Planning target volume (PTV) margins (Prescribing, Recording and Reporting Photon Beam Therapy 1999) are the most widely used method to account for geometric and/or setup uncertainties. In the past, larger PTV margins were used to compensate for setup errors. This resulted in healthy normal tissues receiving unnecessary radiation doses. With advent and increasing popularity of IMRT, highly conformal dose distribution is possible, and accurate target delineation and treatment dose delivery are of particular importance (Hong et al. 2005; Houghton et al. 2009). IGRT is expected to improve the patient-positioning precision and therefore the effectiveness of cancer treatment by targeting and/or tracking tumor more accurately.

Current IGRT routine is to image the patient prior to treatment delivery. Acquisition of pretreatment imaging on a regular basis allows us to assess more detailed treatment information, such as patient's immobilization, range of organ movement, changes in tumor size and shape, etc. The IGRT imaging process can be used as a regular quality assurance method to record the effect of changes in immobilization and other interventions (Dawson and Sharpe 2006). With daily IGRT imaging, interventions to reduce errors and/or generate a new adaptive plan might be implemented sooner, leading to an overall improvement in quality of treatment.

Secondly, current advanced radiotherapy planning, including three-dimensional conformal radiotherapy (3DCRT) and IMRT, produces plans in which high-dose radiation conforms tightly around the target, with reduced doses to healthy tissues, allowing possible dose escalation to the tumor. Such advanced planning has called for highly accurate dose delivery.

Thirdly, IMRT is associated with a steep dose falloff outside the target, calling for stringent requirements for control of geometric uncertainties (such as setup error and organ motion) and a need for enhanced target delineation at planning and target localization before treatment delivery. Geometric uncertainties and day-to-day variability in tumor position emphasize the need for image guidance in conjunction with IMRT.

In addition, the importance of IGRT has increased tremendously with growing interests of stereotactic body radiotherapy (SBRT). SBRT (Lo et al. 2010) is a novel technique and attracts growing interests for many treatment sites, such as the lung, liver, prostate, et al. (Lo et al. 2010; Fakiris et al. 2009; King et al. 2013). SBRT delivers high doses to (relatively) small targets in fewer numbers of fractions (five or fewer), which requires a high degree of confidence in tumor localization provided by high-quality imaging for accurate treatment delivery. Imaging at the time of treatment is needed to ensure that radiotherapy is delivered as intended as the number of fractions reduces.

Technological developments allow radiation delivery to be gated to a specific phase of respiration or to track targets that move because of breathing, thus reducing the volume of healthy tissues that are irradiated. With these strategies to decrease organ motion, frequent imaging of the tumor during radiation delivery is needed to ensure that the intended target volume is treated.

Volumetric and temporal imaging during radiotherapy also provides an opportunity to adapt the changes in the tumor or healthy tissues that arise during a course

of treatment, which otherwise were not apparent without IGRT. Such interventions can potentially lead to further clinical gains. Tumor sites at which such benefits are most likely include those that tend to recur locally rather than distantly, cancers in which increased dose has been associated with enhanced tumor control, lesions adjacent to dose-limiting healthy tissues, and cancers that change in position from day to day.

5.3 Currently Available Image-Guided Techniques

With the advent of fractionated radiation therapy, the patient-positioning reproducibility and uncertainty became a concern. The importance of accurate radiation delivery has been discussed theoretically and demonstrated clinically. The consequences of missing the target are a reduction in tumor control probability and an increase in normal tissue complication probability.

Many technologies have been developed and employed to help ensure the accurate placement of a treatment field (Verellen et al. 2008; Killoran et al. 1997; Marks et al. 1974; Hunt et al. 1995; Herman et al. 2000; Kutcher et al. 1994; Goitein et al. 1975), such as megavoltage (MV)- and/or kilovoltage (kV)-based radiographic 2D planar and volumetric IGRT approaches, non-radiographic approaches, etc. Many solutions have multiple features and continuously evolve into new applications.

5.3.1 2D Planar IGRT Approaches

Portal imaging using film was the standard for patient localization in the 1980s (Kutcher et al. 1994). X-rays or gamma rays were used to develop large-format radiographic films for inspection. The disadvantages of using film imaging are time-consuming, labor intensive, and reimbursed for only one port film verification per week (Herman et al. 2000). The electronic portal imaging device (EPID) gradually replaces the portal imaging using films in the 1990s and became the most widespread planar IGRT technology. The EPID provides a more efficient and effective method for determining radiation field placement accuracy. Various technologies used in EPID have been detailed in literatures (Goitein et al. 1975; Falco et al. 1998). Early array systems used diodes, scintillators, or liquid-based ion chambers. Early fluoroscopic systems were the precursors of the screen-mirror systems used today. Present commercial systems are replaced by flat-panel detector arrays (Falco et al. 1998; Munro 1995; Antonuk et al. 1998), which offer better resolution and faster response.

5.3.2 Volumetric IGRT Approaches

Various volumetric IGRT technologies became clinically available in the early 2000s (Verellen et al. 2008). The first way to visualize 3D anatomy soft tissue prior to treatment and to define the spatial relationship between target and organs at risk is diagnostic CT scanner inside the treatment room. Both the EPID and an orthogonally mounted X-ray imaging device can be used to acquire cone beam volumetric CT data (CBCT). Non-radiographic localization tools are also available, such as ultrasound (US). US devices have been introduced based on the advantage of not requiring a surrogate to visualize the target. On the other hand, these devices can only be used prior to treatment (not during beam on), and it has been argued that this solution is susceptible to interobserver variations and possible introduction of displacement due to pressure of the imaging probe on the patient's lower abdomen. The latest development of adopting introduces MRI in IGRT as it offers superior soft-tissue contrast compared to kV- or MV-based imaging, such as ViewRay system.

5.3.3 Image-Guided Target Delineation

Accurate target definition is vitally important in RT. To be able to "see" the extent of disease more clearly and better define the tumor target volume have been among the most important issues in radiation oncology. Computerized tomography is the most dominant imaging modality and cornerstone in treatment planning, such as (a) the delineation of target and normal structures and (b) quantitative data for tissue heterogeneity (Kijewski and Bjarngard 1978; Chernak et al. 1975). A CT simulation is normally acquired with proper patient immobilization device for patient in the treatment position, referred as the planning CT.

Nowadays, treatment planning relies heavily on the information obtained from CT scan, including high spatial integrity, high spatial resolution, excellent bony structure depiction, and the ability to provide relative electron density information used for radiation dose calculation. The recent development of ultra-fast multi-slice CT has opened a new dimension to CT technology and allows time-resolved (4D) CT imaging of patient's cardiac and breathing cycles. Using array detectors, multi-slice CT scanners can acquire multiple slices simultaneously and thereby greatly increase the speed of CT image acquisition. Currently, all manufactures are providing higher slice CT technology such as 16- and 64-slice CT scanner. The application of 4DCT will be discussed later in this chapter.

In addition to CT, other imaging modalities such as magnetic resonance imaging (MRI), position emission tomography (PET), and/or single-photon emission computed tomography (SPECT) can be acquired and registered with the CT scan to provide additional patient-specific anatomical/functional information that cannot be easily seen from CT image.

MRI is an imaging modality that uses non-ionizing radiation to generate diagnostic and/or treatment images. It uses a powerful magnetic field, radiofrequency

waves, and a computer to create detailed cross-sectional (two-dimensional) and three-dimensional images of the human body. MRI has a wide range of applications in medical diagnosis and treatment planning in many specialties (Magnetic Resonance, a critical peer-reviewed introduction 2013; Hollingworth et al. 2000). MRI and CT are complementary imaging technologies, and each has advantages and limitations for particular applications. The advantages of MRI include:

1. The ability to image without the use of ionizing radiation.
2. The superior soft-tissue contrast than CT scans, especially for the central nervous system (CNS), abdomen and pelvis, etc.
3. The advanced techniques such as diffusion and perfusion MRI, dynamic contrast MRI, MR angiography, MR spectroscopic imaging (MRSI), and functional MRI (fMRI) allow for specific tissue characterization.
4. Functional MRI allows visualization of both active parts of the brain during certain activities, understanding of the underlying networks, etc. It was reported that up to 80% of CNS tumors received improvement in terms of the target volume definition imaged with MRI into the planning process of CNS tumor (http://radiopaedia.org/articles/mri-introduction).

MRI has been widely used in the diagnosis and treatment for tumor delineation purpose. In a clinical setting at radiation oncology, MRI is typically employed together with CT images with the help of image fusion software to delineate the extent of the malignancy. The use of CT and MRI is becoming routine for treatment planning in CNS tumors, etc. Figure 5.1 shows the transverse view of (a) a CT image, (b) a T1-weighted MRI, and (c) a fluid-attenuated inversion recovery (FLAIR) image for a brain tumor.

One of the major issues with MR images in RT is image distortion. MRI technology is moving toward higher field strengths to further improve the MR image quality and the development of some specialized MRI scans (Mundt and Roeske 2006). Diffusion tensor imaging (DTI) (Merboldt et al. 1969; Taylor and

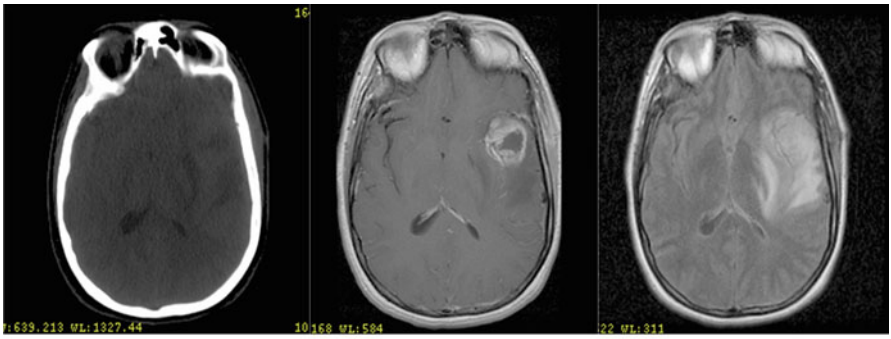

Fig. 5.1 Images of a representative case taken by (**a**) CT, (**b**) T1-weighted MRI, (**c**) FLAIR (Pictures from https://www.aapm.org/meetings/06ss/documents/2006summerschoolIGRTintro_000.pdf)

Bushell 1985), for instance, enables diffusion to be measured in multiple directions and the fractional anisotropy in each direction to be calculated for each voxel. Functional MRI (fMRI) measures signal changes in the brain that are due to changing neural activity. These techniques may allow better definition of brain tumors and better sparing of sensitive regions. Figure 5.1 compares different imaging techniques used in diagnostic and therapeutic applications.

Another imaging approach – positron emission tomography (PET) – has been introduced and now routinely used for RT planning for many disease sites, such as head-and-neck cancer, lung cancer, etc. PET (Bailey et al. 2005) is a functional imaging technique utilizing nuclear medicine to produce a three-dimensional image of functional processes in the body. The system detects pairs of gamma rays emitted indirectly by a positron-emitting radionuclide (tracer), which is introduced into the body on a biologically active molecule. Three-dimensional images of tracer concentration within the body are then constructed by computer analysis. Modern PET scanners are often integrated with CT scanners (so-called PET/CT), which allow PET and CT scans to be performed in immediate sequence during the same session with no need of patient repositioning. This is particularly important for the RT planning purposes (Schwartz et al. 2005; Spratt et al. 2010) so that the PET and CT images can be precisely registered to help delineation and the areas of abnormality on the PET imaging can be more perfectly correlated with anatomy on the CT images.

5.3.4 Image-Guided Treatment Delivery

As the planning target volumes (PTVs) are made increasingly conformal for IMRT, compared with the conventional three-dimensional conformal radiotherapy (3DCRT), the requirements of accurate target delineation and patient setup and its dosimetric coverage during each treatment become increasingly stringent. IGRT makes use of many different imaging techniques ranging from portal imaging, fluoroscopy, ultrasound, to in-room computed tomography systems, etc. In the current context, we classified the available IGRT technologies into three main categories: (A) traditional IGRT technologies, (B) in-room CT-based IGRT technologies, and (C) real-time tracking systems.

5.4 Traditional IGRT Technologies

5.4.1 Portal Imaging

Portal imaging is the acquisition of images with a radiotherapy beam. Traditionally, radiographic films (port films) were placed beyond the patient to produce an image. This method was time-consuming in terms of development and evaluation of the films and was limited to a setup accuracy of about 5 mm (Barry et al. 2012).

The modern era of electronic portal imaging began in the early 1980s (Herman et al., n.d.), and different EPID designs are available using the screen and/or camera imagers, liquid ionization chambers, and solid-state flat-panel detectors (Murphy et al., n.d.). Electronic portal imaging devices (EPIDs), mounted on a Linac using robotic arms, allow for online treatment verification and automatic analysis.

The flat-panel imager is emerging as the new standard detector for portal imaging in IGRT (Herman et al., n.d.). Modern accelerators, such as Varian TrueBeam and Trilogy and Elekta Synergy, are equipped with two kinds of portal imaging systems: (a) kilovoltage X-ray imager in which a conventional X-ray tube is mounted on the gantry with an opposing flat-panel image detector and (b) megavoltage (MV) electronic portal imaging device (EPID) with its own flat-panel image detector. The flat-panel image detector generally is a matrix of 256×256 solid-state detectors consisting of amorphous silicon (a-Si) photodiodes. The kilovoltage (kV) images generally have better contrast than the MV EPID images; both are of sufficiently good quality to visualize soft-tissue targets compared to the kV planning CT. However, the portal images are quite useful in determining the planning target volume in relation to the bony anatomy or implanted fiducials in the target area. Both the kV and MV imager can be used to check patient setup before each treatment as well as online monitoring of target positioning. For kV imager, it can also be used in both the radiographic and fluoroscopy modes to check patient setup before each treatment or to track the movement of fiducial markers due to respiratory motion.

In the past, the most conservative portal is weekly acquisition of images, which is appropriate for treatment plans that are not highly conformal (such as three-dimensional conformal radiotherapy). More precise targeting for the advanced treatment delivery techniques, such as intensity-modulated radiotherapy (IMRT), requests taking portal images daily to assess tumor position variability and systematic setup error, followed by weekly imaging after correction for systematic offsets.

The disadvantages of portal imaging techniques are that (1) the actual treatment target is not clearly defined and the verification is not performed in real time. Therefore, treatment margins are added to the target volumes to accommodate the uncertainty of patient setups and inter- and intra-fractional organ motion; (2) the doses needed for portal imaging is important and varies by application and EPID devices. Improper dose control could result in a useless image and/or extra dose required for obtaining subsequent images; and (3) 3D definition of anatomy information is not available through portal imaging (Fig. 5.2).

5.4.2 Fluoroscopic Imaging

Fluoroscopy is an imaging technique that uses X-rays to obtain real-time moving images of the interior of an object. Conventional fluoroscopic imaging is done at tube voltages between 60 kV and 120 kV. Typical tube currents limited to approximately 100 mA. The tube spectrum is typically filtered by 2–4 mm Al or its

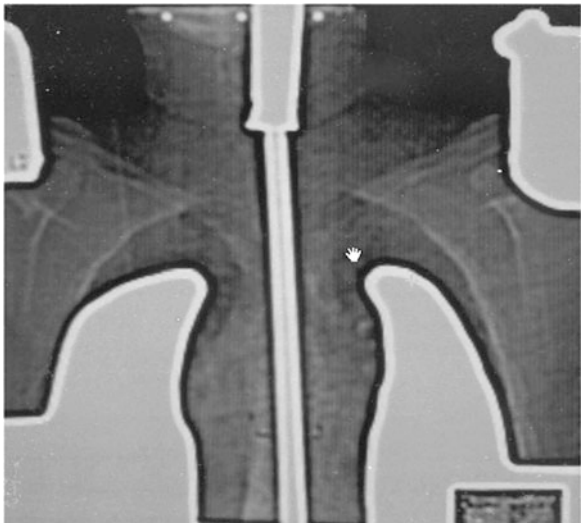

Fig. 5.2 Example of a portal image (Courtesy of Varian Associates, Palo Alto, CA)

equivalent (Leong 1986; Munro et al. 1990; Baily et al. 1980; Antonuk et al. 1996). Fluoroscopy is generally used in (1) pretreatment motion assessment, (2) setup of gating and tracking parameters, and (3) intra-fraction respiratory tracking and compensation. Traditional fluoroscopic system allows the observer to look directly at the phosphor screen to assess tumor motion. The phosphor screen is replaced by digital flat-panel in current design for fluoroscopy-based tracking system. Some of these systems are mounted on the accelerator gantry, while others are installed in the room such as Hokkaido university fluoroscopic system (Chaiken and Lisa 2005). One limitation of fluoroscopy-based tracking systems is the potential for excessive radiation exposure.

5.4.3 Ultrasound

Ultrasound is a noninvasive, non-radiographic real-time imaging technique for localizing soft-tissue structures and tumors, primary in the abdomen, pelvis, and breast. Ultrasound utilizes high-frequency (1 ~ 10 MHz) sound waves to generate anatomical images that have high spatial resolution and tissue characterization discrimination power through image texture analysis. Attached to the BAT system, there is an ultrasound probe mounted on a robotic arm to track the probe's position in space. Ultrasound is the imaging modality widely used in guiding the prostate seed implant procedure; it has been particularly useful to localize the prostate gland in external beam irradiation for prostate. A commonly used ultrasound system is NOMOS B-mode Acquisition and Targeting (BAT) system (NOMOS Corp., Sewickley, PA). Figure 5.3 (a) shows a BAT SXi Ultrasound unit from MONOS

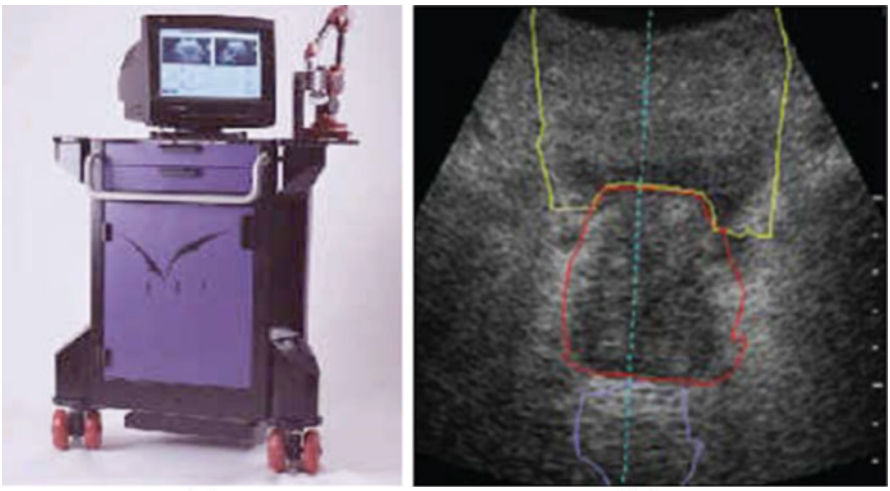

Fig. 5.3 (**a**) A BAT SXi Ultrasound unit from MONOS; (**b**) An Axial ultrasound image with contours overlaid (http://www.nomos.com/pdf/batcam_bro_03.pdf)

and (b) shows an axial ultrasound image with contours overlaid. BAT provides quick ways of localizing prostate before each treatment and making corrections for inter-fraction variations of prostate position (Chaiken and Lisa 2005; BATCAM, n.d.; B-mode Acquisition and Targeting (BAT), n.d.). The pretreatment ultrasound images are fused to the planning CT scans, so the current location of the target volume can be determined in reference to the treatment plan. The patient's position can then be adjusted accordingly so that the target volume is placed precisely and accurately.

The challenges of using ultrasound-guided procedures for localizing prostate are (1) the poor image quality; (2) an unfamiliar appearance of ultrasound images (for many observers), resulting in larger inter- and intra-observer variability (large planning margins have been recommended for ultrasound-guided radiotherapy); and (3) the potential anatomic distortions caused by the transducer pressure on the abdomen for ultrasound-guided prostate therapy. Too much of this pressure could induce a larger shift in the prostate in AP direction of as much as 10 mm (Langen et al. 2003; Peng et al. 2008; Artignan et al. 2004).

5.5 In-Room CT-Based IGRT Modalities

A wide variety of in-room IGRT technologies are available. These in-room CT-based systems provide volumetric anatomic information that is useful for accurate target localization, but also for dose computation that can be used to track the delivered dose distribution. Frequent comparisons of the delivered dose

to the planned dose distribution enable one to make setup corrections or adjust the treatment plan to minimize the variations between the planned and the actual delivered dose, which is the image-guided adaptive radiation therapy (IG-ART).

The advantages of the use of in-room CT-based IGRT technologies include**:**

- 3D definition of anatomy (volumetric imaging) in treatment room.
- Daily CT image can be used for dose calculation (planning or treatment evaluation).
- CT is a mature technology (with minor modifications for radiation therapy applications)
- CT images are widely accepted and familiar by radiation oncologists to determine target volumes and critical organs.
- No direct contact with patient.

5.5.1 CT-on-Rail

A CT-on-rail system integrates a diagnostic CT scanner with a treatment accelerator in RT treatment room. The CT scanner slides on rails in the floor so that the patient does not have to move between the pretreatment scan and treatment. Figure 5.4 shows a Siemens CT-on-rails system at the Department of Radiation Oncology, Medical College of Wisconsin, WI. The Linac and the CT scanner are positioned to the opposite end of the couch. The first integrated clinical system

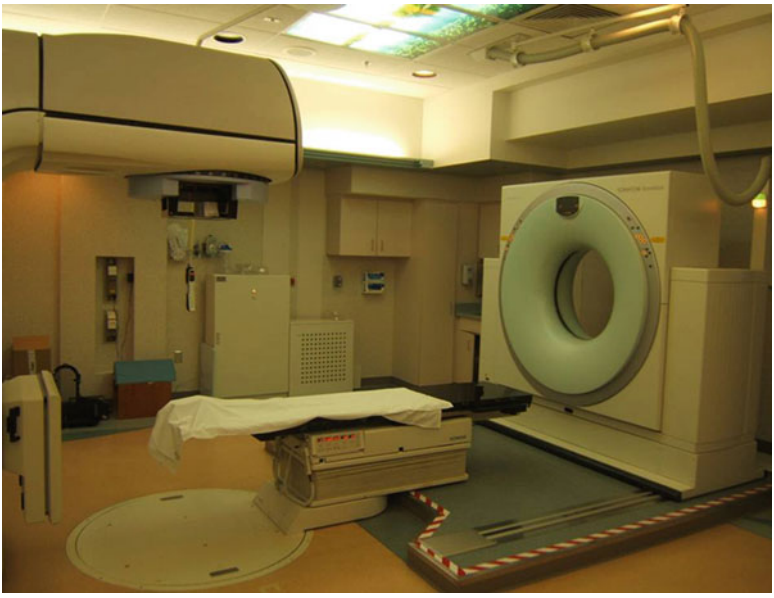

Fig. 5.4 (**a**) A Siemens CT-on-rails system at the Medical College of Wisconsin (Courtesy of Medical College of Wisconisn, Milwaukee, WI)

combining a Linac and an in-treatment-room CT unit was developed by Uematsu et al. in Japan (Uematsu et al. 1996; Kuriyama et al. 2003). The first Siemens CT-on-rails system (PRIMATOM™ Siemens Medical Solutions, Concord, CA) was installed in 2000 at the Morristown Memorial Hospital, Morristown, NJ. The system was equipped with a SOMATOM scanner, which is a single-slice scanner with minimum slice thickness of 1 mm and scan time of 1 s (or less) per rotation. The diameter of the CT gantry is 70 cm, and the FOV is 50 cm in diameter. The speed of the gantry along the rails can vary between 1 mm and 100 mm per second, and the gantry position accuracy is 0.5 mm (Peng et al. 2008). The initial clinical experience with this system was reported by (Ma and Paskalev 2006; Wong et al. 2001; Cheng et al. 2003; Thieke et al. 2006).

The CT-on-rails system allows the quantification and correction of inter-fractional variations between planning and each treatment delivery. To ensure accurate patient positioning, a CT scan is performed immediately before each treatment delivery. After proper patient setup on the couch using in-room lasers, the treatment couch is rotated 180° so that the Linac and the CT gantry are positioned. The pretreatment scan was then registered to the reference image set (the initial planning CT simulation) to verify patient positioning or to determine whether repositioning was required. Due to its diagnostic image quality, the CT-on-rails images were also used to study the anatomical variation during the course treatment.

5.5.2 Kilovoltage Cone Beam CT (kVCBCT)

The on-board kV imaging system provided a choice of imaging modalities of 2D radiographic, fluoroscopic, and 3D cone beam computed tomography (CBCT) imaging. kVCBCT (30–140 kV) imaging systems are commercially available: Varian On-Board Imaging (OBI) (Varian Medical Systems, Palo Alto, CA) and the Elekta XVI Synergy systems (Elekta, Stockholm, Sweden). Figure 5.5 shows pictures of Varian TrueBeam (a) and Elekta Synergy (b), both of which are equipped with kVCBCT systems. Compared to EPIDs, the use of kilovoltage CBCT shows a superior high-contrast resolution (due to the dominance of the photoelectric effect at kV energies) and lower imaging dose to the patients.

The kVCBCT involves acquiring planar projection images from multiple directions as the gantry is rotated through 180° or more. The kV X-ray tube (mounted on a retractable arm) and a kV detector are attached at 90° offset with respect to the central axis of the linear accelerator beam. Images are generated by the flat-panel detectors mounted opposite to the X-ray tube. Three-dimensional volumetric images are reconstructed from these multiple radiographs by the computer using a filtered back-projection algorithm (Feldkamp et al. 1984). The reconstructed CBCT images are fused to the planning CT using automatic or manual registration method to figure out the patient setup error in axial, sagittal, and coronal views; the setup errors will be then adjusted before treatment delivery.

Fig. 5.5 (**a**) Varian TrueBeam accelerator (Varian Oncology Systems, Palo Alto, CA). (**b**) Elekta Synergy (Elekta Inc.). Both accelerators are equipped with kilovoltage imaging systems capable of 2D planar radiography, fluoroscope, and cone beam CT modes

Compared to conventional kVCT images, kVCBCT images have increased artifacts and reduced contrast due to photon scatter (Srinivasan et al. 2014; Yang et al. 2007). However, kVCBCT imaging has shown great soft-tissue contrast and spatial resolution for soft-tissue-based setup, but the image quality can be affected by the acquisition parameters. Figure 5.6 shows a fusion of a planning CT and a kVCBCT of a prostate patient image on Elekta X-ray volume imaging (XVI) system.

5.5.3 Megavoltage Cone Beam CT (MVCBCT)

Another commercially available CBCT imaging system is the Siemens MVision system (Siemens Medical Solutions, Malvern, PA) (Pouliot et al. 2005; Morin et al. 2005). MVCBCT is made using the traditional EPID with the amorphous silicon (a-Si) flat-panel detectors (optimized for MV X-ray). The X-ray source is the megavoltage therapy beam of the accelerator (i.e., 6 MV). Planar projection images are acquired from multiple directions as the X-ray source and the detector rotate around the patient. Figure 5.7 shows a Siemens Primus accelerator equipped with megavoltage cone beam CT (MVCBCT) capability at the department of radiation oncology at UCLA.

To acquire MVCBCT images, the users need to create CBCT imaging protocols by specifying the following parameters: (1) the total dose for a CBCT acquisition (2–60 monitor units [MU]), (2) the reconstruction size (128, 256, or 512), (3) the reconstruction slice interval (1, 2, or 3 mm), (4) source to image distances (SID), etc. By default, the Linac gantry rotates in a continuous 200° arc (270°–110°, clockwise), acquiring one portal image for each angle. This acquisition procedure

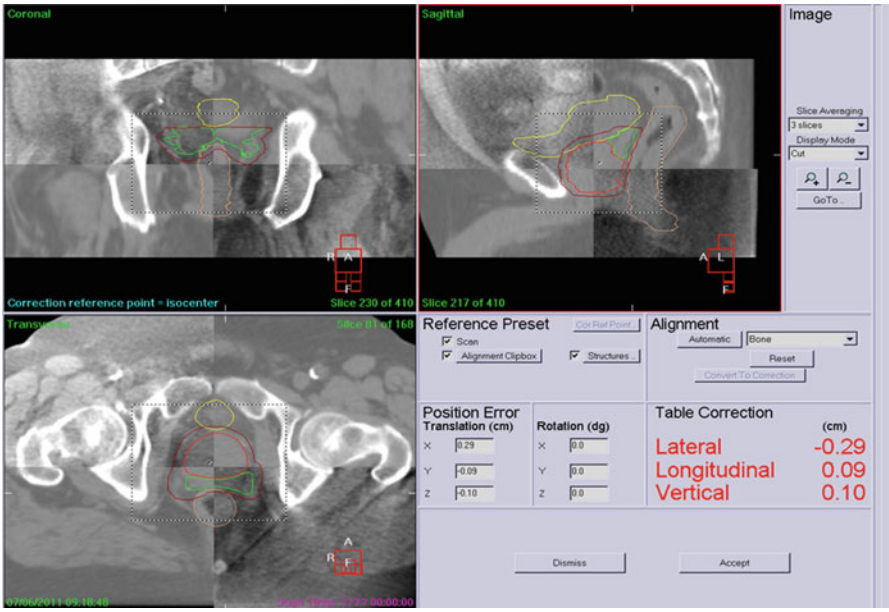

Fig. 5.6 A fusion of a planning CT and a kVCBCT of a prostate patient image on Elekta X-ray volume imaging (XVI) system. Registration can be done automatically or manually using axial, sagittal, and coronal views

Fig. 5.7 A Siemens Primus accelerator equipped with megavoltage cone beam CT (MVCBCT) capability at the department of radiation oncology at UCLA

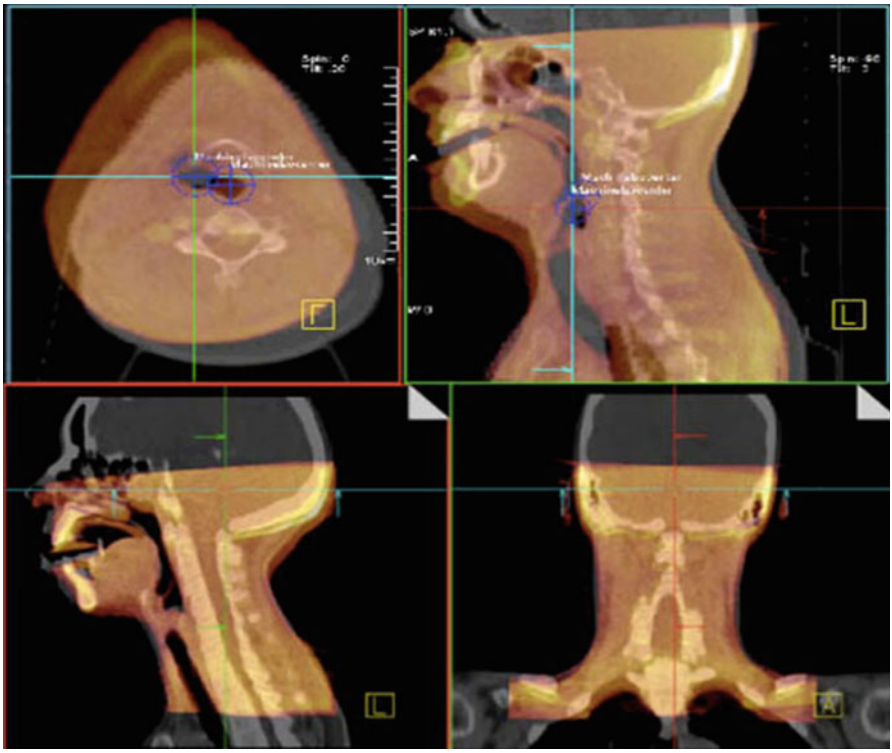

Fig. 5.8 Image registration of a reconstructed MVCBCT image to the planning CT (Courtesy of Jean Pouliot, PhD)

lasts ~45 s. An integrated computer workspace provides automated acquisition of projection images, image reconstruction, MVCBCT image to planning CT registration, and couch shift calculation. The image reconstruction starts immediately after the acquisition of the first portal image, and a typical 256 × 256 × 274 reconstruction volume (1.1 × 1.1 × 1.0 mm^3 voxel size) is completed in 110 s.

Figure 5.8 shows the image registration of a MVCBCT (brown) to the planning CT (gray). The system demonstrates submillimeter localization precision and sufficient soft-tissue resolution to visualize structures such as the prostate (Morin et al. 2005)

Compared to the kVCBCT image, the soft-tissue contrast in the MVCBCT is reduced due to the dominance of Compton scattering. The advantages of kVCBT over MVCBCT can be summarized below:

- Better contrast and spatial resolution
- Better soft-tissue visibility at much lower doses
- Compatibility of kVCBCT images with the reference treatment plan images for patient setup verification and correction

- Combination of radiography, fluoroscopy, and CBCT capabilities from the same source and detector, which provides great flexibility in implementing the goals of IGRT

The potential advantages of MVCBCT over kVCBCT are as summarized as follow:

- Less susceptibility to imaging artifacts due to mental objects such as hip implants, dental fillings, and surgical clips.
- No need for extrapolating attenuation coefficients from diagnostic (kV beams) to the therapeutic beam. CT numbers in MVCBCT correlate directly with electron density.
- The known dose distribution characteristics of the therapeutic beam allow more accurate calculation of imaging dose in the MVCBCT acquisition process.
- Implementation of MVCBCT does not require extensive modifications of a linear accelerator that is already equipped with an EPID.

5.5.4 Megavoltage Fan Beam CT (MVCT)

Helical TomoTherapy Hi-Art System (Accuray Inc., Sunnyvale, CA) is an integrated system that combines CT scanning technology with radiation therapy delivery. Figure 5.9 shows (a) a helical tomotherapy treatment unit and (b) schematic view of tomotherapy hardware components. The actual treatment beam from the linear accelerator is used as the X-ray source for image acquisition with detuned energy of 3.5 MV. The megavoltage fan beam is collimated to a length of 1 mm and

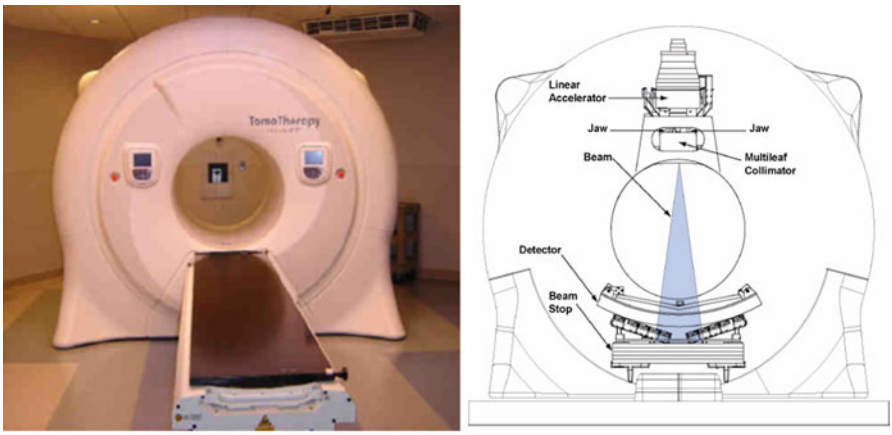

Fig. 5.9 (**a**) The helical tomotherapy treatment unit and (**b**) schematic view of tomotherapy hardware components (Courtesy of Tomotherapy Inc.)

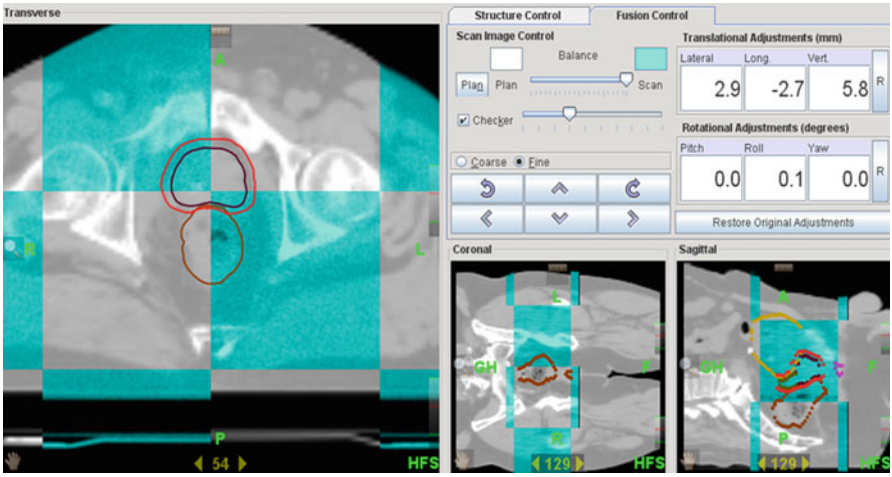

Fig. 5.10 Image registration on tomotherapy operating console

a width of 40 cm at isocenter for MVCT scan. The image reconstruction pixel matrix is defaulted at 512 × 512 with the FOV of 40 cm. Three clinical MVCT acquisition modes (fine, normal, and coarse) are available for (2, 4, and 6 mm) slice thickness, respectively. Tomotherapy is unique in its use of megavoltage computer tomography (MVCT) to guide the radiation treatment based on patient anatomy for that day via a fan beam.

Incorporating a CT scanner with a linear accelerator, the tomotherapy system features image-guidance capability in IG-IMRT using rotational fan beam. The on-board CT system can be used (a) to verify tumor's precise size, shape, and location and patient's setup immediately before or during the treatment to ensure accurate dose delivery, (b) to verify the leaf positions during treatment, (c) to evaluate the actual dose delivered to the patient (as compared to the planned dose), and (d) to adapt the original plan based on the daily image for subsequent fractions (if necessary). Generally, pretreatment MVCT scan takes 2–5 min depending on the scan length with additional imaging doses of 1.0–3.0 cGy. Fig. 5.10 shows Tomo MVCT image registration on tomotherapy operating console.

The MVCT in therapeutic range has less Z-dependence because of the increased Compton and pair-production interactions. Whereas, diagnostic imaging is generally performed at kilovoltage (kV) range which is dominant by the photoelectric interactions, resulting in good contrast resolution due to large atomic number (Z) dependence. Figure 5.11 shows the axial images for head-and-neck case with dental fillings for (a) kVCT scan and (b) MVCT image obtained on a tomotherapy unit. Tomotherapy's MVCT image allows visualization of soft tissues around metal (such as teeth filling and /or hip replacement) and more accurate dose calculation. Compared with the diagnostic kVCT scan, the uniformity and spatial resolutions of

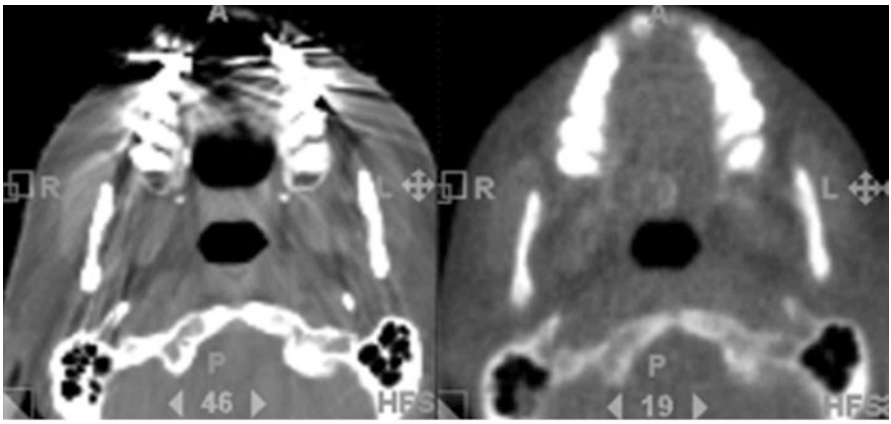

(a) (b)

Fig. 5.11 The axial images for a head-and-neck case with dental fillings. A kVCT planning image is shown on the left (**a**), and a MVCT image obtained on a tomotherapy unit is shown on the right (**b**). The severe streaking aberrations introduced by metal artifacts are clearly seen in kVCT image (Courtesy of Tomotherapy Inc.)

MVCT images generated by the tomotherapy are comparable to that of diagnosis CT images (Meeks et al. 2005; Hong et al. 1999; Forrest et al. 2004) but MVCT has inferior contrast resolution.

The pretreatment MVCT scan can also be used to perform dose verification (Kapatoes et al. 1999; Kapatoes et al. 2001a; Kapatoes et al. 2001b; Langen et al. 2005). The actual dose distribution delivered can be superimposed onto the daily images of the patient obtained at the time of treatment. The results can be compared with the planned isodose on the planning CT. This comparison may be used as an accurate basis for adaptive radiotherapy (ART) whereby the optimized delivery is modified before subsequent fractions.

5.6 Real-Time Tracking Systems

Detecting the tumor position is the most important and challenging task in real-time tracking. Currently, there are four possible means of locating the tumor during treatment: (1) real-time imaging of the tumor itself via, e.g., fluoroscopy; (2) real-time imaging of artificial fiducial markers implanted in the tumor; (3) inference of the tumor position from surrogate breathing motion signals; and (4) - non-radiographic tracking of an active or passive signaling device implanted in the tumor. All of these methods are currently under development or used clinically (Keall et al. 2006).

5.6.1 ExacTrac System

The Brainlab (Brainlab AG, Feldkirchen, Germany) provides versatile IGRT platform for all treatment sites for different imaging procedures. The Brainlab ExacTrac X-ray IGRT system uses a combination of optical positioning and kV radiographic imaging to accurately position patients and make online positioning corrections. The ExacTrac IGRT system is mainly an integration of two subsystems: (1) an infrared (IR)-based optical positioning system (ExacTrac) and (2) a radiographic kV X-ray imaging system (X-ray 6D). The infrared system consists of 2 IR cameras, which are used to monitor reflective body markers placed on the patient's skin to assist in patient initial setup, and an IR reflective reference star, which is attached to the treatment couch and assist in couch movement with spatial resolution to better than 0.3 mm (Jin et al. 2008). The radiographic kV devices consist of two oblique X-ray imagers to obtain high-quality radiographs for patient position verification and adjustment. In addition, the infrared markers provide a respiratory signal for tracking and gating of the treatment beam, with the X-ray system providing periodic confirmation of patient position relative to the gating window throughout treatment (Figs. 5.12 and 5.13).

ExacTrac 6.0 or later version (Jin et al. 2008; ExacTrac, Image-guided radiotherapy BrainLab, n.d.) also provides the possibility to perform 6D patient positioning based on kVCBCT images taken on a Varian OBI. The volumetric kVCBCT datasets will be automatically fused to the pretreatment CT images. The remote-controlled treatment couch and robotic module allow for any shifts to the detected and compensated from outside the treatment room. In July 2010, Brainlab announced the availability of ExacTrac® Infrared Monitoring, an add-on device to existing treatment machines for monitoring patient positioning during radiation therapy treatments. The Brainlab's new technology uses infrared tracking to continually monitor the patient's position and check the reference position for a wide range of treatment disease sites, including the cranial, head and neck, prostate, lung, liver, and spine. ExacTrac offers high-resolution stereoscopic X-ray imaging that targets tumors and corrects patient positioning with submillimeter precision in a quick and automated 2-min setup. The radiation delivered to the patient during imaging is negligible compared to cone beam CT or 2D MV portal images (ExacTrac, Image-guided radiotherapy BrainLab, n.d.).

5.6.2 CyberKnife

The CyberKnife Robotic Radiosurgery System (Accuray Inc., Sunnyvale, CA) is a frameless image-guided system that is specifically designed to deliver stereotactic body radiation therapy (SBRT) (also known as radiosurgery). The system includes a compact lightweight linear accelerator (6 MV) mounting on a true robotic manipulator, allowing for treatment beams deliver from thousands of

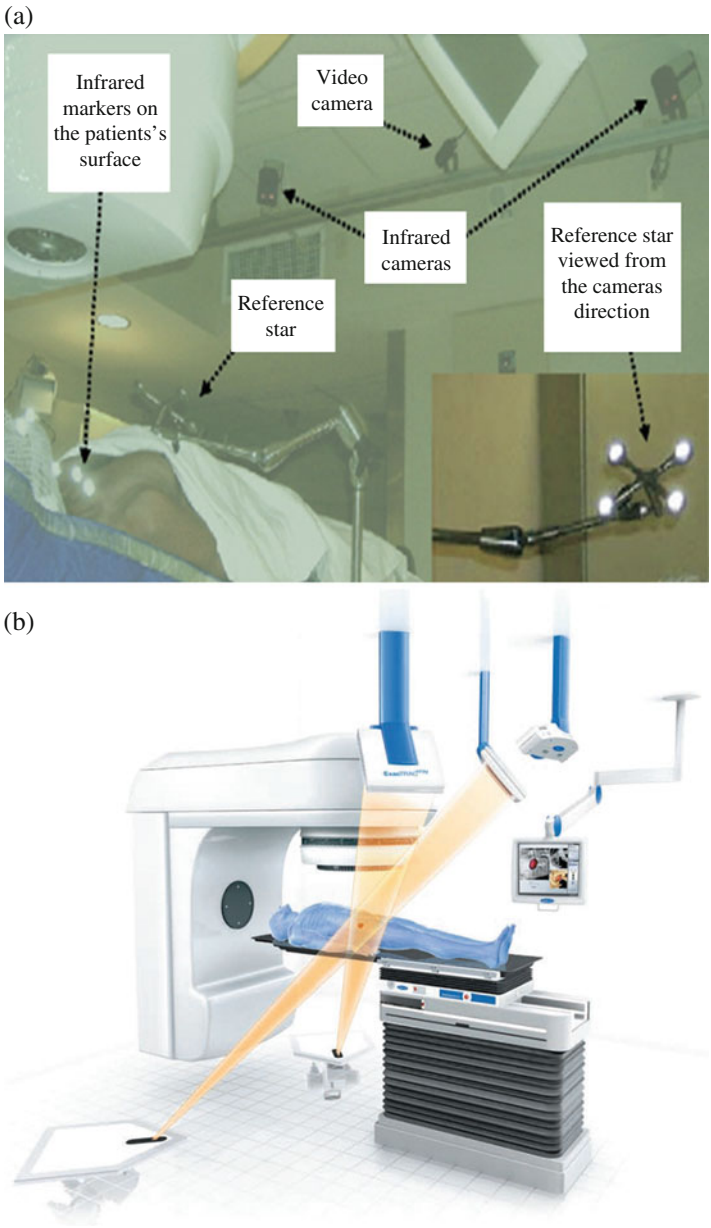

Fig. 5.12 (**a**) The infrared camera-based ExacTrac system; (**b**) the Novalis body image-guided system showing the X-ray imaging devices (Jin et al. 2008)

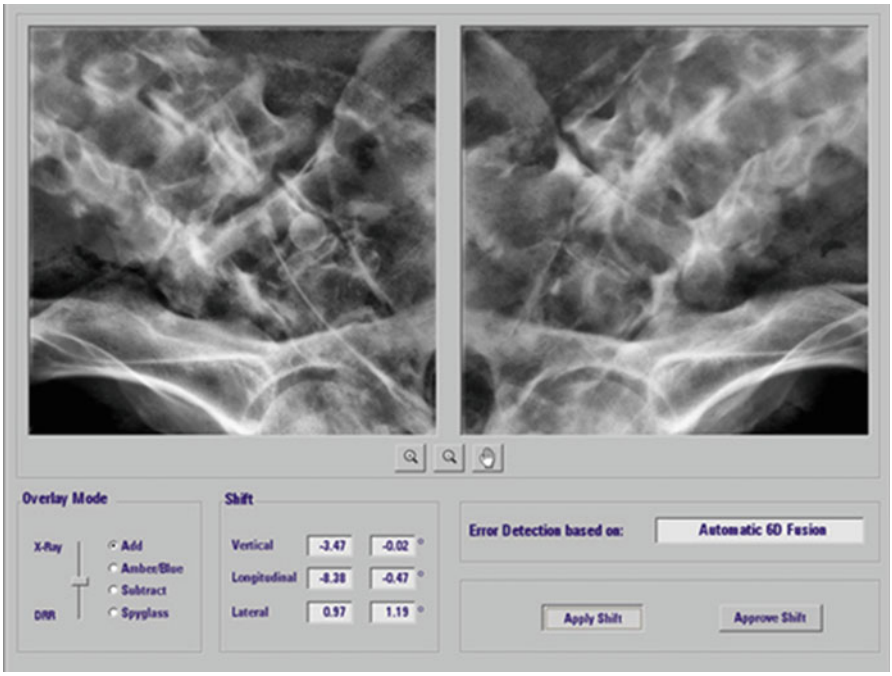

Fig. 5.13 ExacTrac images from a Novalis system (http://www.ofunachuohp.net/rt/machine.html)

non-coplanar, isocentric, or non-isocentric angles. The system provides a noninvasive alternative to surgery for the treatment of both cancerous and non-cancerous tumors anywhere in the body, including the prostate, lung, brain, spine, liver, pancreas, breast, etc. (Gibbs 2006; Nuyttens and van de Pol 2012; Coste-Manière et al., n.d.; Gerszten et al. 2003; Dieterich and Pawlicki 2008). Prior to and/or during treatment, the two diagnostic (kV) X-ray sources and digital amorphous silicon detectors provide a continuous update of the tumor motion and automatically correct the aims of the treatment beam when movement is detected. The CyberKnife system was invented by an American neurosurgeon at Stanford University named John R. Adler (Adler et al. 1997). The system was approved for clinical use by the US Food and Drug Administration in 2001.

Figure 5.14 illustrates the CyberKnife radiosurgery system in a treatment room. The imaging system consists of two orthogonal diagnostic X-ray sources mounted to the ceiling paired with amorphous silicon detectors to acquire live digital radiographic images of the tumor or tumor surrogates. This system allows the robotic manipulator to correct for changes in patient position during treatment beam delivery. In addition, the system equipped a real-time optical tracking subsystem for dynamic compensation of tumor movement due to respiration during

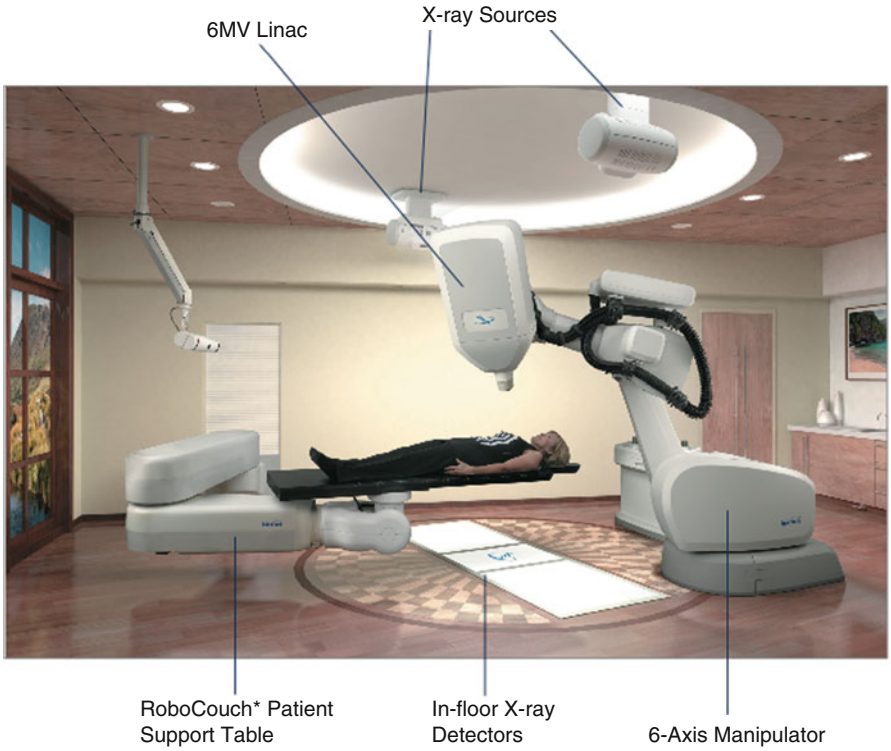

Fig. 5.14 The CyberKnife Robotic Radiosurgery System Stereotactic Radiosurgery system (Picture from http://www.cyberknifelatin.com/pdf/brochure-tecnico.pdf)

treatment delivery. The moving tumors can be treated with a high degree of accuracy while patients breathe normally.

Using its unique robotic mobility and continuous image guidance, the CyberKnife® System is capable of acquiring images for precision patient setup and tracking tumor motion in real time throughout the treatment. The system tracking capabilities eliminate the need for gating techniques and restrictive head frames, providing greater comfort for the patient.

Besides, the CyberKnife treatment delivery software provides an automatic, intuitive user interface to efficiently control all interactions between the robotic manipulator, treatment couch, and imaging system. Treatments have excellent tumor coverage, steep dose gradients, and tight dose conformality, regardless of target shape. The software quickly and automatically processes live images acquired throughout treatment at user-defined intervals, calculates offsets based on digitally reconstructed radiographs (DRRs), and sends offset data to the robotic manipulator for immediate and automatic motion compensation.

5.6.3 ViewRay System

The ViewRay™ system (ViewRay Inc., Oakwood Village, OH) is a unique medical device for radiation treatment that integrates a MRI system (MRIS) with a cobalt-60 (Co-60) radiation treatment machine. The system is specifically designed for MRI-guided radiation therapy with real-time tracking capability (ViewRay system Brochure, n.d.; Operator's manual for ViewRay system 3.5 2014).

Unlike the CT-based IGRT treatment units, the ViewRay system combines the superior imaging capabilities of MRI and RT machine to further optimize IMRT and IGRT and does not introduce additional ionizing radiation to patients. The ViewRay MRI system is a 0.35 T horizontal field MRI, which provides superior soft-tissue contrast and allows for continuously volumetric tracking of soft-tissue targets. If the tumor or critical structures move beyond a physician-defined boundary, the treatment beams automatically pause; when the structure moves back into the target zone, treatment automatically resumes *(ViewRay system Brochure,* n.d.*)*. Physicians can set both spatial and time thresholds for pausing treatment delivery, controlling for the motion of a patient's organs based on real-time 4D MRI data.

Other highlighted features of the ViewRay system include (ViewRay system Brochure, n.d.):

- Three Co-60 sources housed in shielding heads mounted on a ring gantry.
- Each Co-60 source equipped with computer-controlled multileaf collimator (MLC) for IMRT delivery.
- Dynamic images for real-time tracking when the treatment beams are on.
- An operator console for MRI acquisition, patient positioning, dose prediction and re-optimization, and real-time tumor tracking.
- Integrated treatment planning and delivery software for creating treatment plans and managing the treatment delivery process (Fig. 5.15).

Figure 5.16 displays the image registration on a ViewRay system. The primary image set is shown a rectangle. One can fuse MRI, CT, and PET images on the ViewRay system. There are three modes of registration available, including manual rigid registration, automatic rigid registration, and automatic deformable registration (Operator's manual for ViewRay system 3.5 2014)

5.6.4 Calypso 4D Localizing System

The Calypso system (Varian Medical Systems, CA) is a state-of-the-art imaging system designed for real-time tumor tracking for more precision radiation delivery. It combines real-time imaging and external beam radiation therapy to keep the radiation beam precisely focused on the moving target and minimizes damage to surrounding healthy tissue and lessens related side effects commonly associated with cancer radiation treatment. Figure 5.17 shows Calypso electromagnetic field real-time tracking system (Calypso, Varian Medical Systems, CA).

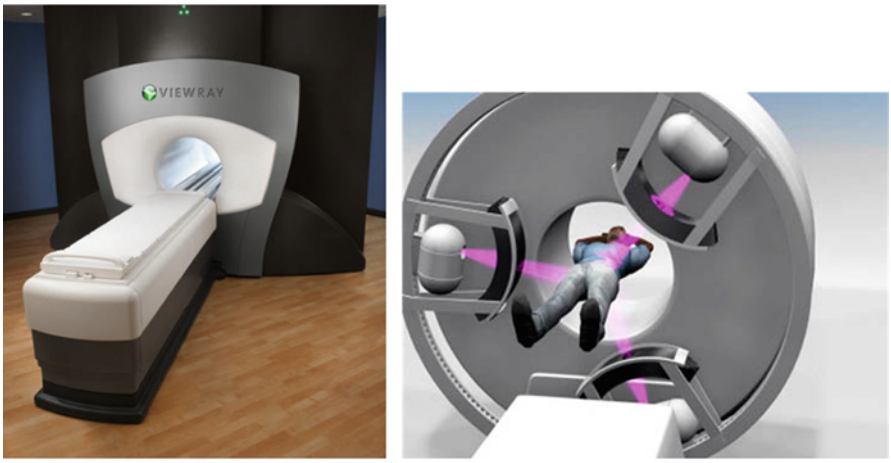

Fig. 5.15 (**a**) The ViewRay treatment unit and (**b**) a schematic of real-time MRI-guided soft-tissue imaging and volumetric tracking system (ViewRay Inc., Oakwood Village, OH) (Courtesy of ViewRay Inc.)

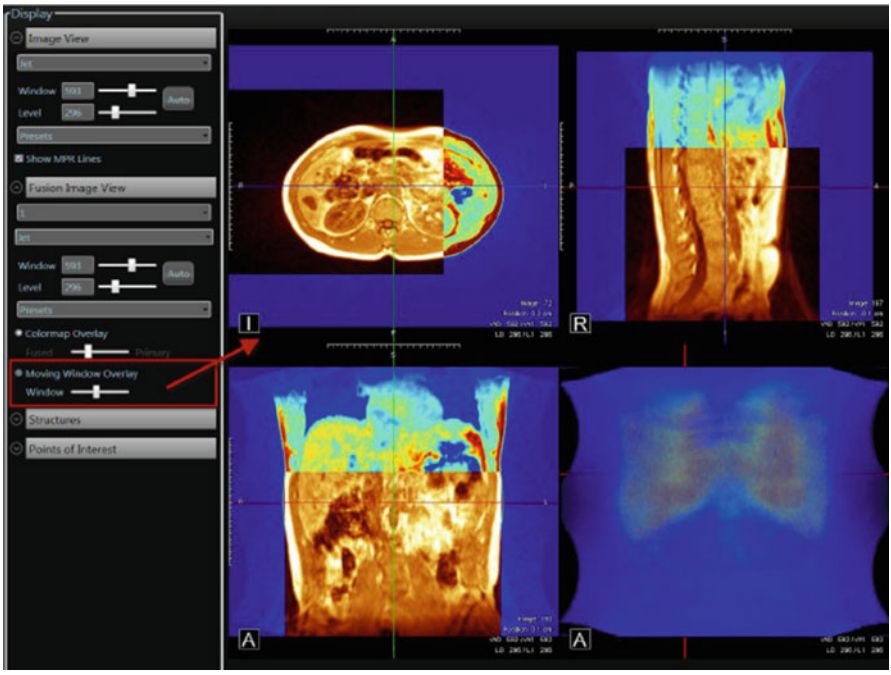

Fig. 5.16 The image registration on a ViewRay system. The primary image set is shown a rectangle (Operator's manual for ViewRay system 3.5 2014)

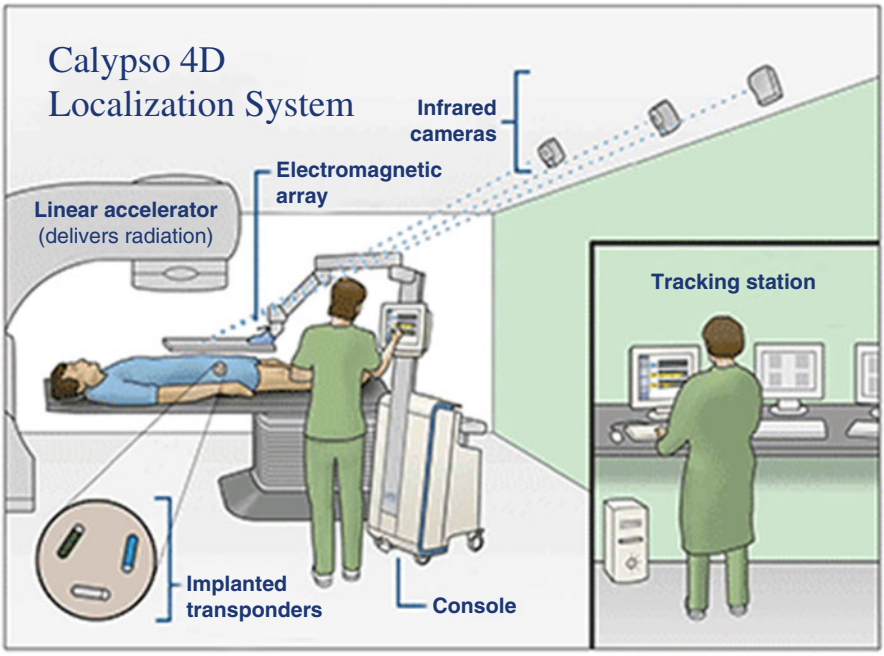

Fig. 5.17 The electromagnetic field real-time tracking system (Calypso, Varian Medical Systems, CA). Figure from https://www.massey.vcu.edu/patient-care/methods/radiation/therapies/calypso

Prior to radiation treatment, three electromagnetic transponders (in mms) called beacons are inserted in or near the tumor to monitor exact tumor motion using safe radiofrequency waves. During treatment, the transponders relay a constant signal, pinpointing the tumor's exact location. Outside the treatment room, a control computer displays the positional information and alerts therapists if and/or when the tumor or organ moves during treatment. No additional ionizing radiation will be needed for target tracking. The approach is feasible for monitoring of tumor position during radiation delivery (Balter et al. 2005) for numerous tumors such as prostate cancer.

5.7 Management of Imaging Dose

Volumetric CT-based IGRT technologies have emerged as the new paradigm for patient positioning, target localization, and external beam alignment in radiotherapy (Murphy et al. 2007). One problem with X-ray-based IGRT technologies is the potential for excessive imaging dose to the patients. Given the imaging procedure is performed on daily basis and repeated throughout the entire treatment fractions (up to 30 or 35 fractionations), imaging doses to patient may be excessive and result

Table 5.1 Comparison of various commercially available CT-based IGRT systems [AAPM TG 179]

CT-based IGRT system	Elekta XVI	Varian OBI	Siemens Artiste	Tomotherapy	Siemens Primatom
Imaging modalities	kV-CBCT	kV-CBCT	kV-CBCT	MV-FBCT	CT-on-rails
Field of view (cm)	50 × 50 × 25.6	45 × 45 × 17	40 × 40 × 27.4	40	50
Imaging dose (cGy)	0.1–3.5	0.3–2.0	3–10	0.7–3.0	0.05–1
Accuracy (mm)	<1	<1	<1	<1	<1
Image acquisition and reconstruction time (min)	2	1.5	1.5	5 s/slice	3 slice/s

in unnecessary toxicity for sensitivities structures. Furthermore, X-ray imaging irradiates a significantly larger region than the treatment volume, and therefore doses to critical structures may be even larger. The general rule for dose management is summarized by as low as reasonably achievable (ALARA) (Murphy et al. 2007).

Many literatures including the AAPM Task Group 75 have analyzed and reported the imaging dose for a number of IGRT protocols (Murphy et al. 2007; Bissonnette et al. 2012; Chan et al. 2011; Stutzel et al. 2008; Moseley et al. 2012). Table 5.1 shows the comparisons of various commercially available CT-based IGRT systems (Bissonnette et al. 2012). Improved image quality is achievable at higher doses for most commercial systems. However, image quality is to be judged based on the critical endpoint of the IGRT process – targeting. It is recommended that dose management techniques that decrease the ionizing radiation imaging dose without affecting targeting be implemented whenever possible (Murphy et al. 2007)

5.8 Image Registration and Correction Strategies

Image registration (Zitova and Flusser 2003) is the process of transforming multimodality images into a same coordinate system for a same target taken at different times. The registration geometrically aligns two images, including the reference (or source) and target images, to compare or integrate the information obtained from different image modalities. Image registration is important for treatment planning stage (i.e., target definition) and treatment delivery stage (i.e., patient alignment). Under the context of image-guided treatment delivery, the reference image generally refers to the planning CT, and the acquired daily images are the target images. Image registration may be challenging because of variability of patient's positioning for every modality and movement of internal organs. Often used image registration algorithm classification includes:

5.8.1 Single- vs Multimodality Methods

The CT images are the most widely used image modalities in radiation oncology; there is growing interests in adopting other image modalities, such as MRI, PET, etc. for better targeting. Single-modality methods tend to register images of the same modality acquired by the same scanner type, while multimodality registration methods tended to register images acquired by different scanner types. Multimodality registration methods are often used in medical imaging as images of a subject are frequently obtained from different scanners. Examples include registration of brain CT/MRI images, whole body PET/CT images for tumor localization, and registration of ultrasound and CT images for prostate localization in radiotherapy.

5.8.2 Rigid vs Deformable Image Registration

Rigid transformations are defined as geometrical transformations including translations and rotations. These transformations typically preserve the point-to-point distance, straightness of lines, and angles between straight lines. Registration problems that are limited to rigid transformations are called rigid registration (Fitzpatrick and West 2001). For example, the shape of a human brain changes very little with head movement, so rigid body registration can be used to fuse different head positions for different scans.

However, rigid alignment does not model anatomic changes from, e.g., organ deformation, patient weight loss, or tumor shrinkage. Nonrigid or deformable image registration (DIR) was developed to account for anatomic changes by finding the mapping between points in one image and the corresponding point in another image. DIR has the perspective of being widely integrated into many different steps of the radiotherapy process, such as treatment planning, treatment delivery (registration between the planning CT and treatment CT) for dose accumulation and contour propagation, etc. (Brock et al. 2006).

5.8.3 Automatic vs Manual Registration

Registration methods may also be classified according to the level of automation, such as automatic, interactive, and manual registration methods. Manual methods provide tools to align the images manually. Interactive methods reduce user bias by performing certain key operations automatically while still relying on the user to guide the registration. Automatic methods do not allow any user interaction and perform all registration steps automatically. The automatic registration algorithms based on mutual information algorithm (Ruchala et al. 2002; Pluim et al. 2003) were adopted for tomotherapy MVCT and Siemens MVCBCT and edge-matching algorithm (Borgefors 1988) adopted by Elekta kVCBCT.

5.8.4 Intensity-Based vs Feature-Based Registration

Image registration involves spatially registering the target image(s) to align with the reference image. The planning CT images are normally referred to as the reference, and the other pretreatment image modalities, such as cone beam CTs, etc., are, respectively, referred to as the target images. Intensity-based methods compare intensity patterns in images via correlation metrics, while feature-based methods find correspondence between image features such as points, lines, and contours (Goshtasby 2006). Intensity-based methods register entire images or sub-images. If sub-images are registered, centers of corresponding sub-images are treated as corresponding feature points. Feature-based methods establish a correspondence between a number of especially distinct points in images. Knowing the correspondence between a number of points in images, a geometrical transformation is then determined to map the target image to the reference images, thereby establishing point-by-point correspondence between the reference and target images.

5.8.5 Online and Offline Correction Strategies for Patient Positioning

There are two basic correction strategies used while determining the most beneficial patient position and beam structure (Jaffray et al. 1999): online and off-line correction. Both serve their purposes in the clinical setting and have their own merits. A combination of the both strategies is often employed. Often, a patient will receive corrections to their treatment via online strategies during their radiation session.

The online correction strategy acquires images prior to the treatment and makes treatment interventions during the current treatment session. The purpose of an online approach is to control and reduce both systematic and random errors. Online correction strategy usually requires a high level of integration of both software and hardware and fast speed.

The off-line correction strategy, however, acquires images before treatment and makes a match to a reference image off-line (i.e., without the patient on the couch). The purpose of the strategy is to reduce the magnitude of the individual patient systematic setup error and, when combined with other patient setup data treated under the same protocol, to calculate the population systematic error. The population-based systematic error is the standard deviation of the systematic errors of all patients within the treated population. Published off-line correction protocols that are widely used are the shrinking action level (SAL) and the no action level (NAL) protocols (National radiotherapy implementation group report 2012; Bel et al. 1993; de Boer et al. 2005; Qi et al. 2013b).

5.9 Clinical IGRT Workflow

The utility of IGRT allows for the verification of patient's anatomy and alignment through relatively low-dose CT imaging prior to each treatment delivery. In general, the IGRT workflow can be summarized as the following steps (Qi et al. 2013a; b):

5.9.1 Initial Patient Setup

Prior to each treatment fraction, appropriate patient alignement need to be ensured using patient-specific marks and/or tatoos to the in-room laser positions. To achieve proper reproducibility during radiotherapy treatment, external immobilization devices are often used and attach to the couch top in a unique position to avoid daily variation in patient repositioning. Figure 5.17 shows a customized head-and-neck and shoulder thermoplastic mask that was generally used to provide immobilization of the entire upper part of the body in the treatment position. Immobilization devices not only help the patient maintain the required consistent position but may also achieve an advantageous treatment position to reduce dose to normal tissue. However the benefit of these devices can be affected by the skill of the clinical staff making and/or positioning the devices and the cooperation of the patient. The most vital component of an accurate and reproducible treatment position is that the patient is comfortable, and the position can be easily reproduced by both therapeutic radiographer and patient (Fig. 5.18).

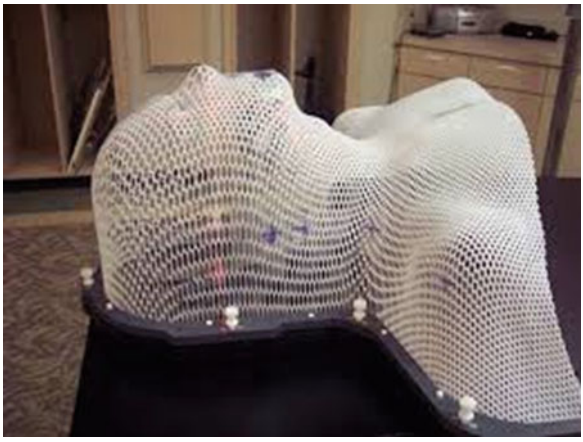

Fig. 5.18 Immobilization devices of head-and-neck and shoulder thermoplastic mask for H&N radiotherapy

5.9.2 Image Acquisition and Registration

The pretreatment IGRT image, such as CBCT or MVCT, is acquired in the treatment position immediately before each treatment delivery. The daily scans are then registered to the reference image set (the planning CT scan) on the treatment console to verify patient positioning or to determine discrepancies. The initial registration is normally done automatically and followed by manual adjustments if necessary. A rigid image alignment is generally performed initially in order to supply a suitable starting point for estimation of organ deformation for deformable registration.

5.9.3 Compensation for Patient Misalignment

Make appropriate shifts to compensate for patient misalignments. The adjustments are sent to the treatment unit and the couch shifts automatically to compensate for the differences.

Manual alignment is the most reliable and intuitive approach for volume alignment. However, manual alignment is subject to interobserver subjectivity/variations. When relatively large adjustments were required (i.e., >1 cm), the physician is called to verify the alignment on the treatment console.

5.10 Image Guided Adaptive Treatment (IG-ART)

Adaptive radiotherapy (ART) has been introduced as a feedback control strategy to include patient-specific treatment variation explicitly in the control of treatment planning and delivering during the treatment course (Yan 2008, 2010). Specifically, ART is referred to change the radiation treatment plan delivered to a patient during a course of radiation treatment to account for (1) temporal changes in anatomy (i.e., tumor volume changes, weight loss or gain, etc.) and (2) changes in tumor biology/function, etc. ART aims to adjust the treatment plan, with the aid of frequent (i.e., daily) image guidance, when the plan quality degrades. Various ART strategies were developed, such as off-line between fractions, online immediately prior to a fraction, and/or in real time during a fraction.

The integration of the image-guidance system into the radiation delivery system, such as OBI on Varian, XVI on Elekta, and MVCT image acquisition detector on tomotherapy, allows for image acquisition on a daily basis. These daily images ensure the accuracy of patient setup for every treatment, allowing the physician to check size, location, and the shape of the tumor before each treatment and compare that day's image with the treatment plan. This assures that the radiation treatment is directed at the tumor site and allows for modification of the treatment plan if

necessary, which, in turn, brings a higher level of precision and accuracy to cancer treatment. In addition, the actual dose delivered to the patient can be calculated based on daily volumetric CT scan. This delivered dose can be directly compared with the planned dose distribution to trigger a re-optimization process if necessary.

A representative application for using daily CT is to assess the tumor volume changes during the treatment course. The significant tumor volume changes as revealed from daily CT scans have been reported (Li et al. 2007) for a soft-tissue sarcoma case at the chest region. The CTVs for the sarcoma were contoured on a series of daily MVCT sets and were compared with the CTV and PTV obtained from the planning kVCT scan. Figure 5.19 (a) shows the inter-fractional variations

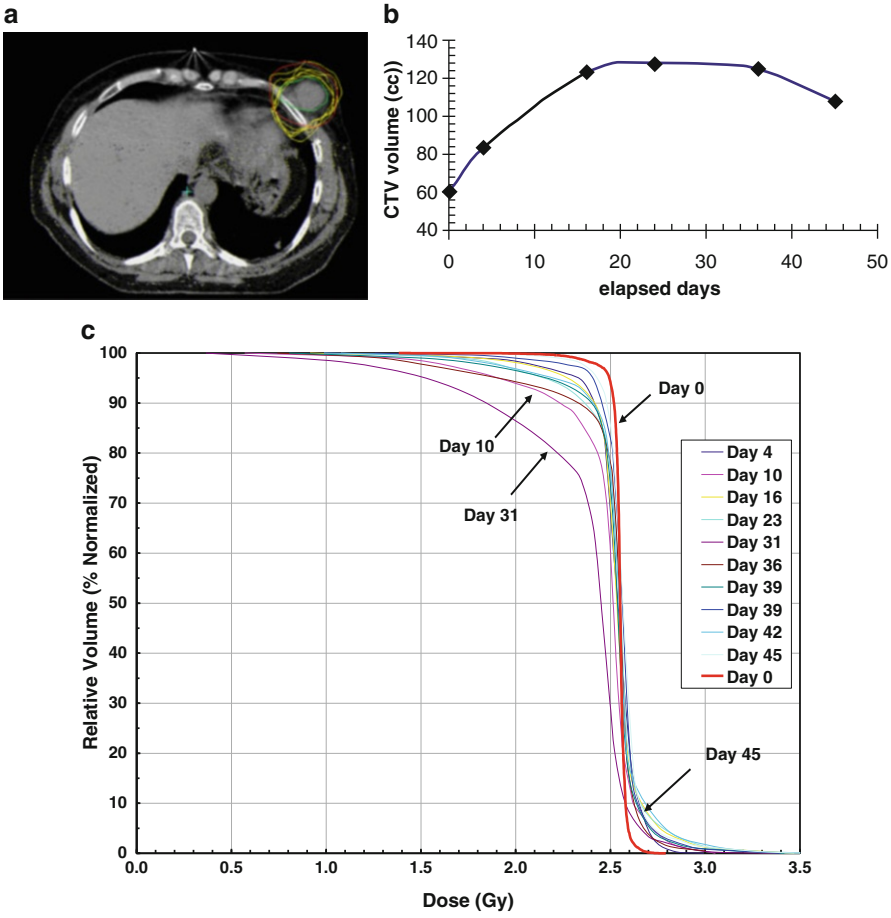

Fig. 5.19 The inter-fractional variations for a sarcoma case at chest region (Li et al. 2007). (**a**) The inter-fractional variations of daily CTV (*yellow*) contoured from daily MV CT, as compared with the planning CTV (*green*) and PTV (*red*) and overlaid on an axial kVCT image. (**b**) Variation of clinical target volume (CTV) during treatment course. Clinical target volume (in cubic centimeters) for each data point (e.g., at a given treatment-elapsed day) is indicated. (**c**) The verification DVHs based on given MVCT images and the planning DVH for PTV

of daily CTV (yellow) contoured from daily MVCT, as compared with the planning CTV (green) and PTV (red) and overlaid on an axial kVCT image. Figure 5.19 (b) displays quantitative variations of the daily CTVs during the treatment course. The CTV (in cubic centimeters) at a given elapsed day is indicated. It is clear that the CTV at the middle course of treatment was approximately doubled from the planning CTV (Day 0). The original PTV was not big enough to cover the enlarged daily CTVs. The verification DVHs based on given MVCT images were calculated and compared to the planning DVHs (Day 0) (Fig. 5.19 (c)). The significant tumor volume changes result in dramatic underdosing for PTV, e.g., the PTV coverage varies from 30% to 95% which depends on the given treatment factions.

The ART is an appealing concept that aims to adjust the treatment plan based on the anatomical changes assessed on a daily basis using pretreatment volumetric images (Schwartz et al. 2012; Castadot et al. 2010a; Castadot et al. 2010b; Nishi et al. 2013; Wu et al. 2009; Lee et al. 2008; Chen et al. 2014). Due to the flexibility of the head-and-neck region, radiation response often causes tumor and normal organ shrinkage and patient weight loss during their treatment course. Patient physiologic and anatomic variations cannot be fully accounted for and can cause the delivery doses of the tumor and normal organ to degrade from their initial planning dose distribution.

Despite marked advances in RT, radiation often causes significant functional deficits for the head-and-neck patients. Of particular importance for H&N cancer RT are the parotid glands. High-radiation doses to the parotid glands leads to xerostomia, where the patient's ability to swallow and eat is significantly degraded (De Meerleer et al. 2000). Wu et al. (Wu et al. 2009) reported that the dosimetric benefit of replanning with reduced margins could result in up to 30% parotid gland dose sparing. Lee et al. (Lee et al. 2008) reported an average of 15% parotid mean dose difference between the delivered vs the planned doses due to anatomic changes during a course of radiation treatment. Recently, Schwartz et al. (Schwartz et al. 2012) performed a prospective adaptive trial for a group of 24 H&N cancer patients with 1–2 replan(s) in the middle of the treatment course. The early outcomes indicated promising clinical outcome results including low initial toxicity and high disease control. Chen AM (Chen et al. 2014) also concluded that ART conveys a significant benefit in appropriately selected patients with H&N cancer. However, clinical implementation of ART remains challenging and labor intensive due to the complexity and lack of robustness in automated image registration/segmentation/dose summation.

Qi et al. (2015) presented a clinical application of a near real-time automated framework that could help decision-making process for adaptive planning to account for plan quality degradation for a group of H&N cases. A quantitative patient-specific biomechanical H&N anatomic model (Neylon et al. 2015) assembled using the conventional CT simulation (to account for subject specific sub-anatomy locations) is employed to register in real time with routine on-board CT (to monitor the effects of posture/physiologic variations in gross treatment volume). Such an automated framework will streamline the process of an accurate determination of the daily and integrated delivered dose for adaptive radiation therapy for H&N cases.

5.11 Management of Respiratory Motion

Respiratory motion can introduce significant errors in the external beam radiation therapy for patients with thoracic, abdominal, and pelvic tumors (Keall et al. 2006). The problems of unaccounted respiratory motion in radiotherapy can be summarized in the following aspects:

1. Image acquisition. Respiratory motion can generate artifacts for all image modalities, such as CT and PET, both of which are considered to be standard-of-care image modalities for lung cancers. Respiratory motion-induced artifacts can lead to difficulties in delineating target boundaries.
2. Treatment planning (Chen et al. 2004; Nehmeh et al. 2003; Caldwell et al. 2003; Balter et al. 1996; Ford et al. 2003). Target movement and patient setup uncertainty are generally accounted for using a planning margin. Larger treatment margins are generally needed to cover the limits of the moving targets, which is suboptimal. Since larger margin calls for larger radiation field size, resulting in larger volume of healthy tissues exposed to radiation doses. This increased treatment volume increases the likelihood of treatment-related complications. However, if the margins are not sufficiently large, part of the CTV will not receive adequate dose coverage resulting in potential tumor recurrence. The artifacts observed in CT images make it challenging to quantify the magnitude of margin (to allow for respiratory motion) particularly for individual patients in whom a wide range of tumor motion is observed.
3. Radiation delivery. Radiation delivery in the presence of intra-fraction organ motion causes an averaging or blurring of the static dose distribution over the path of the motion. This displacement results in a deviation between the intended and delivered dose distributions.

Precise geometric knowledge of the target volume is needed for treatment planning to better achieve therapeutic goal. Typically, a patient's radiotherapy plan is based on conventional CT scans. However, this conventional CT scan is only a "snapshot" of the patient and tumor position, i.e., it is acquired on 1 day and at one time. Patient and/or tumor changes can either occur daily (inter-fraction motion) or during the treatment delivery (intra-fraction motion). Besides, such conventional CT scan can include severe motion artifacts that result from interplay between the advancing scan plane and object motion. It has been recognized that severe artifacts can be introduced if organ motion is present during CT acquisition (Rietzel et al. 2005).

Although tumor displacement varies depending on the site and organ motion, it is most prevalent and prominent in lung cancers. To explicitly include organ/target motion in treatment planning and delivery, time-resolved 4D computed tomography (4DCT) is needed.

5.11.1 Four-Dimensional Computed Tomography (4DCT)

A common approach to obtain high-quality CT data in the presence of respiratory motion is time-resolved 3D CT imaging, often referred to as 4DCT. Generally, the 4DCT scan process includes two steps: (1) to acquire a set of CT images per slice through the volume and (2) to sort the images and assemble spatiotemporally coherent datasets from the data acquired (Xing et al. 2006). The 4DCT images essentially create a video sequence of how the tumor moves during the breathing cycle. The 4DCT provides clinicians with more data to determine the mean tumor position, tumor range of motion, tumor range of motion for treatment planning, etc.

4DCT data are normally acquired on a multi-slice CT scanner in axial or helical mode during normal breathing. Respiration signals during 4DCT scanning are acquired using surrogate signals such as the motion of the abdominal surface, internal anatomy, or volume of air measured by spirometer during inhalation and exhalation cycles. Varian Real-time Position Management (RPM) system (Varian Medical Systems, Palo Alto, CA) using an external respiration signal is widely adopted at clinical setting. The RPM system consists of an infrared source, a CCD camera, and a reflective plastic box (with two infrared-reflecting dots) (Fig. 5.20). The reflective box is usually placed on the anterior abdominal surface, typically midway between the xyphoid process and the umbilicus, and the exact position is chosen to maximize the anteroposterior (AP) motion. The motion is captured by the camera and analyzed in real time by RPM system on a computer connected to the RPM camera. A patient undergoing a 4DCT scan on a GE scanner is shown in Fig. 5.20a. The system captures the position of the abdominal surface as a function of time during respiration (Fig. 5.20a). The breathing pattern is recorded for the duration of the scan and is referred to as the "respiratory trace" (Fig. 5.20b). Once the 4DCT acquisition has finished, the software retrospectively computes the phase at each point of the respiratory trace by determining the location of the peaks at end-inspiration and assigning percentages to inter-peak points based on a linear interpolation of the peak-to-peak distance (so-called phase sorting). 4DCT Images are acquired at each couch position for many respiratory phases. Normally, each image is sorted into one of ten phase bins, and the phase bins are selected to be evenly spaced in time over the respiratory cycle. Under this scheme, end-inspiration occurs at 0%, while end-expiration typically appears near 50%. A 4DCT dataset may involve as many as 1000–2000 CT slices. The peak-to-peak distance, the position of end-expiration with respect to end-inspiration can vary between respiratory cycles.

The 4DCT dataset allows for the generation of individualized internal target volumes (ITVs) for treatment planning but also allows for the retrospective selection of phases for gated radiotherapy (Mageras et al. 2004; Underberg et al. 2005). The maximum intensity projection (MIP), defined as the highest data value encountered along the viewing ray for each pixel of volumetric data, giving rise to a full intensity display of the brightest object along each ray on the projection image. MinIP projections reflect the lowest data value encountered along the viewing ray for each pixel of volumetric data (Li et al. 2006). However, there are some unsolved issues in 4DCT (Xing et al. 2006; Pan et al. 2004; Pan 2005).

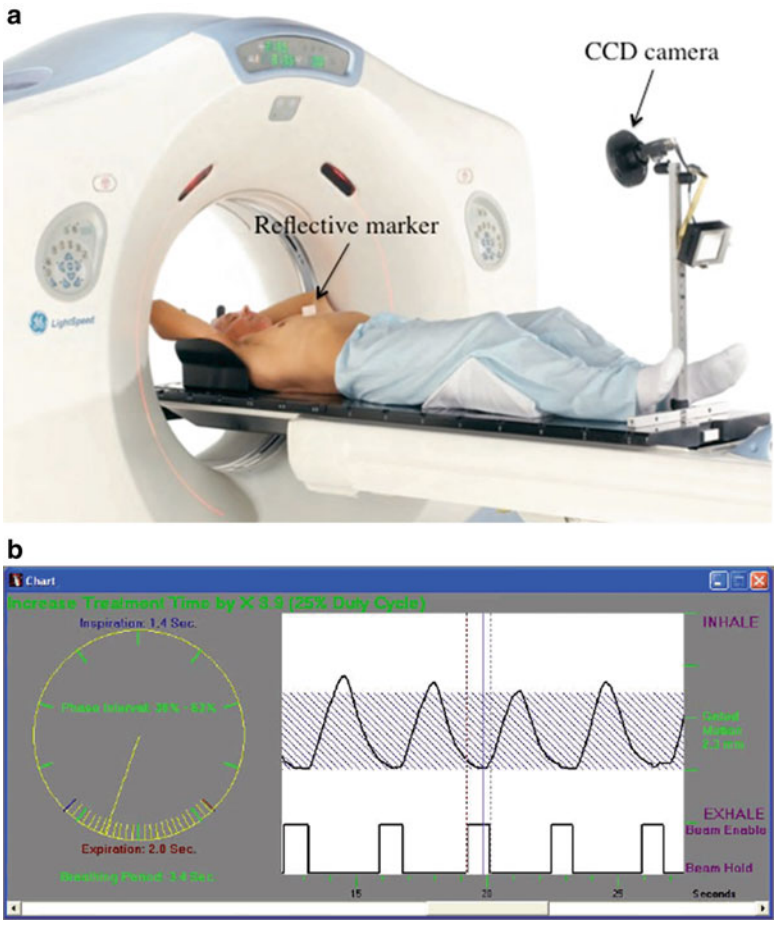

Fig. 5.20 (**a**) System setup for a 4DCT scan. (**b**) Respiratory waveform using an infrared-tracking camera and a reflective marker on Varian RPM system

5.11.2 Methods to Account for Respiratory Motion in Radiotherapy

A variety of treatment delivery techniques were developed to reduce the impact of respiratory motion in radiotherapy (Keall et al. 2006; Li et al. 2006). These techniques can be broadly stratified into the following four categories:

1. Respiratory gating methods. Respiratory gating involves the administration of radiation within a particular portion of the patient's breathing cycle (Keall et al.

2002; Kubo and Hill 1996), commonly referred to as the "gate." The position and width of the gate within a respiratory cycle are determined by monitoring the patient's respiratory motion, using either an external respiration signal or internal fiducial markers. Gated procedures are longer than non-gated procedures since the beam is turning on/off.

2. Breath-hold methods. The technique delivers radiation during a breath hold and predominantly applied to lung and breast radiotherapy. There have been several techniques developed, e.g., deep inspiration breath hold (Hanley et al. 1999; Wong et al. 1999) active breathing control (Wong et al. 1999) and self-held breath hold (Kim et al. 2001).
3. Forced shallow-breathing techniques. The technique employs a pressure plate against the abdomen in a reproducible fashion to minimize diaphragmatic excursions, thereby reducing breathing motion (Lax et al. 1994; Negoro et al. 2001).
4. Respiration synchronized techniques (such as real-time tumor tracking). Real-time tumor tracking dynamically shifts the radiation dose in space so as to follow the tumor's changing position during free breathing (Neicu et al. 2003; Shirato et al. 2000; Murphy 2004). In principle, real-time tracking can be achieved by using an MLC or a linear accelerator attached to a robotic arm or, alternatively, by aligning the tumor to the beam via couch motion. Under ideal conditions, continuous real-time tracking can eliminate the need for a tumor-motion margin in the dose distribution while maintaining a 100% duty cycle for efficient dose delivery (Keall et al. 2006).

Due to the concern regarding patient tolerance and compliance, as well as the availability of technology, the respiratory gating is, by far, the most clinically acceptable method to account for respiratory motion in radiation therapy. During a gating treatment, the computer synchronizes the beam with the respiratory cycles and switches the beam on only at the certain phases of respiration cycle. Typically, the gating interval is centered at end-expiration because of the increased reproducibility at this point and spans 20%–30% of the breathing period to provide a reasonable duty cycle. Treatment plans are optimized for this phase range by planning on an averaged composite of the scans within the interval. Gating treatment normally takes longer time to deliver the treatment due to treatment beam was turned on/off at some phases.

5.12 Conclusion

The importance of image-guided radiation treatment has increased tremendously for the IMRT and/or SBRT. Development of imaging technologies allows accurate pretreatment target definition but also patient localization prior to or during each treatment. The use of image guidance allows the tumor and adjacent healthy organs to be visualized to ensure radiation doses are delivered more precisely to the target tumors within the body without compromising health tissue.

IGRT has become a routine procedure of current clinical practice, despite of technical issues still need to be resolved or improved, such as a robust deformable registration method and auto-segmentation of the contours outlined on the planning CT to daily CTs (such as CBCT or MVCT, etc.). In addition, new IGRT technologies, such as MRI-guided radiotherapy, are continuously advancing to the field of radiation oncology. IGRT will continuously play important role in routine clinical practice and lead to better improve clinical outcome.

Questions

1. What is IGRT? Why IGRT is important and particularly important for IMRT?
2. What are the imaging modalities commonly used for target definition of brain tumor in treatment planning?
3. Name some of current available IGRT technologies. What are the advantages and disadvantages for the kilovoltage imagers compared to the megavoltage imagers in general?
4. List some treatment sites that IGRT is generally utlized. Why IGRT is especially helpful for prostate cancer radiotherapy?
5. List advantages of kilovoltage CBCT (kVCBCT) over Megavoltage CBCT (MVCBCT)?
6. What are the tumor site that ultrasound is generally applied to? List advantages and disadvantages of using ultrasound as an IGRT approach. with the use of Ultrasound for IGRT?
7. What are online and off-line correction strategies? The advantages and disadvantages for each strategy?
8. Definition of image registration. Why image registration is important in radiation therapy?
9. What is adaptive therapy? Describe the benefit and challenges of implementation of adaptive radiotherapy in clinical setting.
10. What is 4DCT? What is MIP? Descibe how a 4DCT is acquired and why it is important in radiation treatment.
11. What is potential concern of using CT-based IGRT technologies during radiation treatment?
12. What is real-time tracking? Name some the real-time tracking systems available in current clinical practice.

References

Adler JR Jr et al (1997) The Cyberknife: a frameless robotic system for radiosurgery. Stereotact Funct Neurosurg 69:124–128

Antonuk LE et al (1996) Megavoltage imaging with a large-area, flat-panel, amorphous silicon imager. Int J Radiat Oncol Biol Phys 36:661–672

Antonuk LE et al (1998) Initial performance evaluation of an indirect-detection, active matrix flat-panel imager (AMFPI) prototype for megavoltage imaging. Int J Radiat Oncol Biol Phys 42:437–454

Artignan X, Smitsmans M, Lebesque JV et al (2004) Online ultrasound image guidance for radiotherapy of prostate cancer: impact of image acquisition on prostate displacement. Int J of Radiat Oncol Biol Phys 59(2:595–601

Bailey DL, Townsend DW, Valk PE (2005) Positron emission tomography: basic sciences. Secaucus, Springer-Verlag. Isbn: 1–85233–798-2

Baily NA, Horn RA, Kampp TD (1980) Fluoroscopic visualization of megavoltage therapeutic x ray beams. Int J Radiat Oncol Biol Phys 6:935–939

Balter JM, Ten Haken RK, Lawrence TS, Lam KL, Robertson JM (1996) Uncertainties in CT-based radiation therapy treatment planning associated with patient breathing. Int J Radiat Oncol Biol Phys 36(1):167–174

Balter JM, Wright JN, Newell LJ et al (2005) Accuracy of a wireless localization system for radiotherapy. Int J Radiat Oncol Biol Phys 61:933–937

Barry A, Loredana M, Eva B (2012) Biomedical physics in radiotherapy for cancer. CSIRO Publishers, Collingwood

BATCAM (n.d.) Multi-probe image-guided radiation therapy. http://www.nomos.com/pdf/Batcam_bro_03.pdf

Bel A, van Herk M, Bartelink H, Lebesque JV (1993) A verification procedure to improve patient set-up accuracy using portal images. Radiother Oncol 29(2):253–260. PubMed PMID: 8310153

Bissonnette JP, Balter PA, Dong L, Langen KM, Lovelock DM, Miften M, Moseley DJ, Pouliot J, Sonke JJ, Yoo S (2012) Quality assurance for image-guided radiation therapy utilizing CT-based technologies: a report of the AAPM TG-179. Med Phys 39(4):1946–1963

B-mode Acquisition and Targeting (BAT) Ultrasound for image-guided radiotherapy. Ramer R, May 13, 2005. http://rii.uthscsa.edu/personalpages/lancaster/DI2_Projects_2005/BAT.pdf

de Boer HC, van Os MJ, Jansen PP, Heijmen BJ (2005) 17. Application of the no action level (NAL) protocol to correct for prostate motion based on electronic portal imaging of implanted markers. Int J Radiat Oncol Biol Phys 61(4):969–983

Borgefors G (1988) Hierarchical chamfer matching: a parameter edge matching algorithm. IEEE Trans Pattern Anal Mach Intell 10:849–865

Brock KK, Dawson LA, Sharpe MB et al (2006) Feasibility of a novel deformable image registration technique to facilitate classification, targeting, and monitoring of tumor and normal tissue. Int J Radiat Oncol Biol Phys 64(4):1245–1254

Butler EB, Teh BS, 3rd Grant WH et al (1999) SMART (simultaneous modulated accelerated radiation therapy) boost: a new accelerated fractionation schedule for the treatment of head and neck cancer with intensity modulated radiotherapy. Int J Radiat Oncol Biol Phys 45:21–32

Caldwell CB, Mah K, Skinner M, Danjoux CE (2003) Can PET provide the 3D extent of tumor motion for individualized internal target volumes? A phantom study of the limitations of CT and the promise of PET. Int J Radiat Oncol Biol Phys 55(5):1381–1393

Castadot P, Geets X, Lee JA, Christian N, Gregoire V (2010a) Assessment by a deformable registration method of the volumetric and positional changes of target volumes and organs at risk in pharyngo-laryngeal tumors treated with concomitant chemo-radiation. Radiat Oncol 95:209–217

Castadot P, Lee JA, Geets X, Gregoire V et al (2010b) Adaptive radiotherapy of head and neck cancer. Seminar Radiat Oncol 20:84–93

Chaiken, Lisa MD (2005) B-Mode acquisition and targeting stereotactic ultrasound: the ultimate in Tumor localization for prostate cancer. Cancer Care Center technologies. 13 May 2005. http://www.cancercareconsultants.com/technologies/articles/bmode-chaiken-article.htm

Chan M, Yang J, Song Y et al (2011) Evaluation of imaging performance of major image guidance systems. Biomed imaging Interv J 7:1–7

Chen GT, Kung JH, Beaudette KP (2004) Artifacts in computed tomography scanning of moving objects. Semin Radiat Oncol 14(1):19–26

Chen AM, Daly ME, Cui J et al (2014) Clinical outcomes among patients with head and neck cancer treated by intensity-modulated radiotherapy with and without adaptive preplanning. Head Neck 1:1–6

Cheng CW, Wong J, Grimm L, Chow M, Uematsu M, Fung M (2003) Commissioning and clinical implementation of a sliding gantry CT scanner installed in an existing treatment room and early clinical experience for precise tumor localization. Am J Clin Oncol 26:e28–e36

Chernak ES, Antunez RA, Jelden GL et al (1975) The use of computed tomography for radiation therapy treatment planning. Radiology 117:613

Coste-Manière E, Olender D, Kilby W, Schulz RA (n.d.) Robotic whole body stereotactic radiosurgery: clinical advantages of the cyberKnife® Integrated system. Reprinted by permission from The International Journal of Medical Robotics and Computer Assisted Surgery. http://www.robotics.org/content-detail.cfm/Industrial-Robotics-News/Robotic-Whole-Body-Stereotactic-Radiosurgery: Clinical-Advantages-of-the-CyberKnife®-Integrated-System/content_id/1085

Dawson LA, Sharpe MB (2006) Image-guided radiotherapy: rationale, benefits, and limitations. Lancet Oncol:848–858

De Meerleer GO, Vakaet LA, De Gersem WR, De Wagter C, De Naeyer B, De Neve W (2000) Radiotherapy of prostate cancer with or without intensity modulated beams: a planning comparison. Int J Radiat Oncol Biol Phys 47:639–648

Dieterich S, Pawlicki T (2008) Cyberknife image-guided delivery and quality assurance. Int J Radiat Oncol Biol Phys 71:S126–S130

ExacTrac, Image-guided radiotherapy BrainLab (n.d.) https://www.brainlab.com/wp-content/uploads/2014/01/Brochure-ExacTrac.pdf

Fakiris AJ, McGarry RC, Yiannoutsos CT, Papiez L et al (2009) Stereotactic body radiation therapy for early-stage non–small-cell lung carcinoma: four-year results of a prospective phase II study. Int J Radiat Oncol Biol Phys 75(3):677–682

Falco T, Wang H, Fallone BG (1998) Preliminary study of a metal/a-se-based portal detector. Med Phys 25:814–823

Feldkamp IA, Davis LC, Kress JW (1984) Practical cone-beam algorithm. J Opt Soc AmA 1:612–619

Fitzpatrick JM, West B (2001) The distribution of target registration error in rigid-body point-based registration. IEEE Trans Med Imaging 20:917–927

Ford EC, Mageras GS, Yorke E, Ling CC (2003) Respiration-correlated spiral CT: a method of measuring respiratory-induced anatomic motion for radiation treatment planning. Med Phys 30 (1):88–97

Forrest LJ, Mackie TR, Ruchala K, Turek M, Kapatoes J, Jaradat H, Hui S, Balog J, Vail DM, Mehta MP (2004) The utility of megavoltage computed tomotherapy images from a helical tomotherapy system for setup verification purposes. Int J Radiat Oncol Biol Phys 60 (5):1639–1644

Gerszten PC, Ozhasoglu C, Burton SA, Vogel WJ, Atkins BA, Kalnicki S, Welch WC (2003) Cyberknife frameless real-time image-guided stereotactic radiosurgery for the treatment of spinal lesions. Int J of Radiat Oncol Bio Phys 57(2):S370–S371

Gibbs IC (2006) Frameless image-guided intracranial and extracranial radiosurgery using the Cyberknife™ robotic system. Cancer Radiother 10:283–287

Goitein M, Busse J et al (1975) Immobilization error: some theoretical considerations. Radiology 117:407–12. Boyer AL et al (1992) A review of electronic portal imaging devices (EPIDs). Med Phys 19:1–16

Goshtasby A (2006) Ardeshir, 2-D and 3-D image registration for medical, remote sensing, and industrial applications, Wiley press, 2005. Int J Radiat Oncol Biol Phys 64:1245–1254

Hanley J, Debois MM, Mah D, Mageras GS, Raben A, Rosenzweig K et al (1999) Deep inspiration breath-hold technique for lung tumors the potential value of target immobilization and reduced lung density in dose escalation. Int J Radiat Oncol Biol Phys 45:603–611

Herman MG, Kruse JJ, Hagness CR (2000) Guide to clinical use of electronic portal imaging. JACMP 1(2):38–57

Herman MG, Balter JM, Jaffray DA, McGee KP, Munro P et al (n.d.) Clinical use of electronic portal imaging: report of AAPM radiation therapy committee task group 58. Med Phys 28 (5):712–737

Hollingworth W, Todd CJ, Bell MI, Arafat Q, Girling S, Karia KR, Dixon AK (2000) The diagnostic and therapeutic impact of MRI: an observational multi-centre study. Clin Radiol 55(11):825–831

Hong TS, Welsh JS, Ritter MA, Harari PM et al (1999) Megavoltage computed tomography- an emerging tool for image-guided radiotherapy. Am J of Clinical Oncol 30(6):617–623

Hong TS, Tome WA, Chappell RJ et al (2005) The impact of daily setup variations on head and neck intensity modulated radiation therapy. Int J Radiat Oncol Biol Phys 61:779–788

Houghton F, Benson RJ, Tudor GST et al (2009) An assessment of action levels in imaging strategies in head and neck cancer using TomoTherapy. Are our margins adequate in the absence of image guidance? Clin Oncol 21:720–727

Hunt MA, Schultheiss TE, Desobry GE, Hakki M, Hanks GE (1995) An evaluation of setup uncertainties for patients treated to pelvic sites. Int J Radiat Oncol Biol Phys 32:227–233

http://www.cyberknife.com/uploadedFiles/CyberKnife_Overview/500929.A_CyberKnife_Patient_Brochure_FINAL.pdf (n.d.)

Jaffray DA, Bissonnette JP, Craig T (1999) X-ray imaging for verification and localization in radiation therapy in modern technology of radiation oncology (suppl. 1). Modern technology of radiation oncology. Medical Physics Pub, Madison, WI. Isbn: 0–944838–38-3

Jin JY, Yin FF, Tenn S, Medin PM, Solberg TD (2008) Use of the brainlab exacTrac X-ray 6D system in image-guided radiotherapy. Med Dosim 33:124–134

Kapatoes JM, Olivera GH, Reckwerdt PJ, Fitchard EE, Schloesser EA, Mackie TR (1999) Delivery verification in sequential and helical tomotherapy. Phys Med Biol 4:1815–1841

Kapatoes JM, Olivera GH, Ruchala KJ, Smilowitz JB, Reckwerdt PJ, Mackie TR (2001a) A feasible method for clinical delivery verification and dose reconstruction in tomotherapy. Med Phys 28(4):528–542

Kapatoes JM, Olivera GH, Balog JP, Keller H, Reckwerdt PJ, Mackie TR (2001b) On the accuracy and effectiveness of dose reconstruction for tomotherapy. Phys Med Biol 46:943–966

Keall PJ, Kini VR, Vedam SS, Mohan R (2002) Potential radiotherapy improvements with respiratory gating. Australas Phys Eng Sci Med 25:1–6

Keall PJ, Mageras GS, Balter JM et al (2006) The management of respiratory motion in radiation oncology report of AAPM task group 76. Med Phys 33:3874–3900

Kijewski PK, Bjarngard BE (1978) The use of computed tomography data for radiotherapy dose calculations. Int J Radiat Oncolo Biol Phys 4:429

Killoran JH, Kooy HM, Gladstone DJ, Welte FJ, Beard CJ (1997) A numerical simulation of organ motion and daily setup uncertainties: implications for radiation therapy. Int J Radiat Oncol biol Phys 37:213–221

Kim DJ, Murray BR, Halperin R, Roa WH (2001) Held-breath self-gating technique for radiotherapy of non-small-cell lung cancer: a feasibility study. Int J Radiat Oncol Biol Phys 49:43–49

King CR, Freeman D, Kaplan I, Fuller D, Bolzicco G, Collins S, Meier R, Wang J, Kupelian P, Steinberg M, Katz A (2013) Stereotactic body radiotherapy for localized prostate cancer: pooled analysis from a multi-institutional consortium of prospective phase II trials. Radiother Oncol 109:217–221

Kubo HD, Hill BC (1996) Respiration gated radiotherapy treatment: a technical study. Phys Med Biol 41:83–91

Kuriyama K, Onishi H, Sano N et al (2003) A new irradiation unit constructed of self-moving gantry-CT and Linac. Int J Radiat Oncolo Biol Phys 55:428–435

Kutcher GJ et al (1994) Comprehensive QA for radiation oncology: report of AAPM radiation therapy committee task group 40. Med Phys 21:581–618

Langen KM, Pouliot J, Anezinos C, Aubin M, Gottschalk AR, Hsu IC, Lowther D, Liu YM, Shinohara K, Verhey LJ, Weinberg V, 3rd Roach M (2003) Evaluation of ultrasound-based prostate localization for image-guided radiotherapy. Int J Radiat Oncol Biol Phys 57:635–644

Langen KM, Meeks SL, Poole DO et al (2005) The use of megavoltage CT (MVCT) images for dose recomputations. Phys Med Biol 50:4259–4276

Lax H, Blomgren I, Naslund, Svanstrom R (1994) Stereotactic radiotherapy of malignancies in the abdomen: methodological aspects. Acta Oncol 33:677–683
Lee C, Langen KM, Lu W et al (2008) Assessment of parotid gland dose changes during head and neck cancer radiotherapy using daily megavoltage computed tomography and deformation image registration. Int J Radiat Oncol Biol Phys 71:1563–1571
Leong J (1986) Use of digital fluoroscopy as an on-line verification device in radiation therapy. Phys Med Biol 31:985–992
Li AX, Stepaniak C, Gore E (2006) Technical and dosimetric aspects of respiratory gating using a pressure-sensor motion monitoring system. Med Phys 33:145–154
Li XA, Qi XS, Pitterle M (2007) Interfractional variations in patient setup and anatomic change assessed by daily computed tomography. Int J Radiat Oncol Biol Phys 68:581–591
Lo SS, Fakiris AJ, El C et al (2010) Stereotactic body radiation therapy: a novel treatment modality. Nat Rev Clin Oncol 7(1):44–54
Ma CM, Paskalev K (2006) In-room CT techniques for image-guided radiation therapy. Med Dos 31:30–39
Mageras GS, Pevsner A, Yorke ED et al (2004) Measurement of lung tumor motion using respiration-correlated CT. Int J Radiat Oncol Biol Phys 60:933–941
Magnetic resonance, a critical peer-reviewed introduction. European Magnetic Resonance Forum. Retrieved 16 Nov 2013
Manning MA, Wu Q, Cardinale RM et al (2001) The effect of setup uncertainty on normal tissue sparing with IMRT for head-and-neck cancer. Int J Radiat Oncol Biol Phys 51:1400–1409
Marks JE, Haus AG, Sutton HG, Griem ML (1974) Localization error in the radiotherapy of Hodgkin's disease and malignant lymphoma with extended mantle fields. Cancer 34:83–90
Meeks SL, Harmon JF, Langen KM, Willoughby TR, Wagner TH, Kupelian PA (2005) Performance characterization of megavoltage computed tomography imaging on a helical tomotherapy unit. Med Phys 32(8):2673–2681
Merboldt K, Hanicke W, Frahm J (1969) Self-diffusion NMR imaging using stimulated echoes. J Magn Reson 64(3):479–486
Morin O, Gillis A, Chen J et al (2005) Megavoltage cone-beam CT: system description and clinical applications. Med Dosim 31:51–61
Moseley DJ, Pouliot J, Sonke JJ, Yoo S (2012) Quality assurance for image-guided radiation therapy utilizing CT-based technologies: a report of the AAPM TG-179. Med Phys 39 (4):1946–1963. doi:10.1118/1.3690466
Mundt AJ, Roeske JC (2006) In: Bortfeld T, Schmidt-Ullrich R (eds) Image-guided radiation therapy. Springer, Berlin Heidelberg
Munro P (1995) Portal imaging technology: past. Present and Future Semin Radiat Oncol 5:115–133
Munro P, Rawlinson JA, Fenster A (1990) A digital fluoroscopic imaging device for radiotherapy localization. Int J Radiat Oncol Biol Phys 18:641–649
Murphy MJ (2004) Tracking moving organs in real time. Semin Radiat Oncol 14:91–100
Murphy MJ, Balter J, Balter S et al (2007) The management of imaging dose during image-guided radiotherapy: report of the AAPM task group 75. Med Phys 34:4041–4063
Murphy MJ, Balter J, Balter S, BenComo JA, Das IJ et al (n.d.) The management of imaging dose during image-guided radiotherapy: report of the AAPM task group 75. Med Phys 34 (10):4041–4063
National radiotherapy implementation group report (2012) Image guided Radiotherapy (IGRT) guidance for implementation and use
Negoro Y, Nagata Y, Aoki T, Mizowaki T, Araki N et al (2001) The effectiveness of an immobilization device in conformal radiotherapy for lung tumor: reduction of respiratory tumor movement and evaluation of the daily setup accuracy. Int J Radiat Oncol Biol Phys 50:889–898
Nehmeh SA, Erdi YE, Rosenzweig KE, Schoder H, Larson SM, Squire OD, Humm JL (2003) Reduction of respiratory motion artifacts in PET imaging of lung cancer by respiratory

correlated dynamic PET: methodology and comparison with respiratory gated PET. J Nucl Med 44(10):1644–1648
Neicu T, Shirato H, Seppenwoolde Y, Jiang SB (2003) Synchronized moving aperture radiation therapy (SMART): average tumour trajectory for lung patients. Phys Med 48:587–598
Neylon J, Qi XS, Sheng K, Staton R, Pukala J, Manon R, Low DA, Kupelian P, Santhanam A (2015) A GPU based high-resolution multi-level biomechanical head and neck model for validating deformable image registration frameworks. Med Phys 42(1):232. doi:10.1118/1.4903504
Nishi T, Nishimura Y, Shibata T, Tamura M, Nishigaito N, Okumura M (2013) Volume and dosimetric changes and initial clinical experience of a two-step adaptive intensity modulated radiation therapy (IMRT) scheme for head and neck cancer. Radiother Oncol 106:85–89
Nuyttens JJ, van de Pol M (2012) The CyberKnife radiosurgery system for lung cancer. Expert Rev Med Devices 9(5):465–475
Operator's manual for ViewRay system 3.5 (2014), Document No. L-0009
Pan T (2005) Comparison of helical and cine acquisitions for 4DCT imaging with multi-slice CT. Med Phys 32:627–634
Pan T, Lee T, Rietzel E et al (2004) 4DCT imaging of a volume influenced by respiratory motion on multiple-slice CT. Med Phys 31:333–340
Peng C, Kainz K, Lawton C, Li XA (2008) A comparison of daily megavoltage CT and ultrasound image guided radiation therapy for prostate cancer. Med Phys 35(12):5619–5628
Pluim JP, Maintz JBA, Viergever MA (2003) Mutual-information-based registration of medical images: a survey. IEEE Trans Med Imaging 22:986–1004
Pouliot J, Bani-Hashemi A, Chen J et al (2005) Low-dose megavolt- age cone-beam CT for radiation therapy. Int J Radiat Oncol Biol Phys 61:552–560
Prescribing, recording and reporting photon beam therapy (1999) (Supplement to ICRU Report 50):62
Qi XS, Hu A, Lee SP, Lee P, DeMarco J, Li XA, Steinberg ML, Kupelian P, Low D (2013a) Assessment of interfraction patient setup for head-and-neck cancer intensity modulated radiation therapy using multiple computed tomography-based image guidance. Int J Radiat Oncol Biol Phys 86(3):432–439
Qi XS, Wu ST, Newman F, Li AX, Hu AY (2013b) Evaluation of interfraction patient setup errors for image-guided prostate and head-and-neck radiotherapy using kilovoltage cone beam and megavoltage fan beam computed tomography. J Radiotherapy in Practice 12:334–343
Qi XS, Santhanam A, Neylon J et al (2015) Near real-time assessment of anatomic and dosimetric variations for head-and-neck radiotherapy via a GPU-based dose deformation framework. Int J Radiat Oncol Biol Phys 92(2):415–422
Rietzel E, Pan T, Chen GT (2005) Four-dimensional computed tomography: image formation and clinical protocol. Med Phys 32(4):874–889
Ruchala K, Olivera GH, Kapatoes J (2002) Limited-data image registration for radiotherapy positioning and verification. Int J Radiat Oncol Biol Phys 54:592–605
Schwartz DL, Ford EC, Rajendran J et al (2005) FDG-PET/CT-guided intensity modulated head and neck radiotherapy: a pilot investigation. Head Neck 27(6):478–487
Schwartz DL, Garden AS, Thomas J, Chen YP, Zhang YB et al (2012) Adaptive radiotherapy for head-and-neck cancer: initial clinical outcomes from a prospective trial. Int J Radiat Oncol Biol Phys 83:986–993
Shirato H, Shimizu S, Kitamura K, Nishioka T et al (2000) Four-dimensional treatment planning and fluoroscopic real-time tumor tracking radiotherapy for moving tumor. Int J Radiat Oncol Biol Phys 48:435–442
Spratt DE, Diaz R, McElmurray J et al (2010) Impact of FDG PET/CT on delineation of the gross tumor volume for radiation planning in non-small cell lung cancer. Clin Nucl Med 35(4):237–243
Srinivasan K, Mohammadi M, Shepherd J (2014) Applications of Linac-mounted kilovoltage cone-beam computed tomography in modern radiation therapy: a review. Pol J Radiol 79:181–193

Stutzel J, Oelfke U, Nill S (2008) A quantitative image quality comparison of four differernt image guided radiotherapy devices. Radiother Oncol 86:20–24

Taylor DG, Bushell MC (1985) The spatial mapping of translational diffusion coefficients by the NMR imaging technique. Phys Med Biol 30(4):345–349

Thieke C, Malsch U, Schlegel W, Debus J, Huber P, Bendl R, Thilmann C (2006) Kilovoltage CT using a Linac-CT scanner combination. Br J Radiol 79:S79–S86

Uematsu M, Fukui T, Shioda A et al (1996) A dual computed tomography and linear accelerator unit for stereotactic radiation therapy: a new approach without cranially fixated stereotactic frame. Int J Radiat Oncol Biol Phys 35:587–592

Underberg RWM, Lagerwaard FJ, Slotman BJ et al (2005) Benefits of respiration-gated stereotactic radiotherapy for stage I lung cancer—an analysis of 4DCT data sets. Int J Radiat Oncol Biol Phys 62:554–560

Verellen D, Ridder MD, Storme G (2008) A (short) history of imaged-guided radiotherapy. Radiother Oncol 86:4013

ViewRay system Brochure (n.d.) http://www.viewray.com/product/L0013_RevCMRIdian+Overiew+Brochure-2.pdf

Wong W, Sharpe MB, Jaffray DA, Kini VR, et al The use of active breathing control (ABC) to reduce margin for breathing motion., Int J Radiat Oncol Biol Phys 1999;44:911–919

Wong JR, Grimm L, Uematsu M, et al (2001) Treatment of lung tumor with stereotactic radiation therapy using the world's first PRIMATOM system: a case report. Electromedia 69:127–130

Wu Q, Chi Y, Chen P, Krauss J, Yan D, Martinez A et al (2009) Adaptive replanning strategies accounting for shrinkage in head and neck IMRT. Int J Radiat Oncol Biol Phys 75:924–932

Xing L, Thorndyke B, Schreibmann E et al (2006) Overview of image-guided radiation therapy. Med Dosim 31:91–112

Yan D (2008) Developing quality assurance processes for image-guided adaptive radiation therapy. Int J Radiat Oncol Biol Phys 71:S28–S32

Yan D (2010) Adaptive radiotherapy: merging principle into clinical practice. Semin Radiat Oncol 20:79–83

Yang Y, Schreibmann E, Li T, Wang C, Xing L (2007) Evaluation of on-board kV cone -beam CT (CBCT)-based dose calculation. Phys Med Biol 52(3):685–705

Zelefsky MJ, Fuks Z, Happersett L, Lee HJ et al (2000 Jun) Clinical experience with intensity modulated radiation therapy (IMRT) in prostate cancer. Radiother Oncol 55:241–249

Zitova B, Flusser J (2003) Image registration methods: a survey. Image Vis Comput 21:977–1000